Université Abdou Moumouni

Doctoral Research Program on Climate Change and Energy (DRP-CCE)

NIGER

INTERNATIONAL MASTER PROGRAM IN RENEWABLE ENERGY AND GREEN HYDROGEN

SPECIALITY: ENERGY SYSTEMS ANALYSIS FOR GREEN HYDROGEN TECHNOLOGIES

MASTER THESIS

Topic:

Optimal Sizing of Renewable Powered Green Hydrogen Refuelling Stations for Hydrogen Vehicles Case study: Guinea

Presented on 25th September 2023, by:

Akoi Sakouvogui

Jury Members:

German Supervisor:	Prof. Dr.-Ing. Andrea Benigni Research Center Forschungszentrum Jülich, Germany
Local Supervisors:	Ass. Prof. Mounkaila Saley Moussa Université Abdou Moumouni de Niamey, Niger
	Dr. Souley Kallo Moutari Université Abdou Moumouni de Niamey, Niger
President:	Prof. Nana Sarfo Agyemang Derkyi University of Energy and Natural Resources, Sunyani, Ghana
Examinator:	Dr Hassane Adamou Université Abdou Moumouni de Niamey, Niger

Academic year 2022-2023

DEDICATION

I would like to dedicate this thesis to my beloved mother, Koly KOIVOGUI, who has been a constant source of prayerful support for me. She always blessed me and wished me success in my research. I also want to acknowledge my other family members, particularly my older brother Köva SAKOUVOGUI, who has generously provided financial support throughout my academic journey.

Acknowledgements

First and foremost, I would like to praise and thank God Almighty who has bestowed on me countless blessings, knowledge and opportunities, so that I have been finally able to accomplish the thesis.

Secondly, my efforts aside, this work would have not been possible without the guidance and help of the following people who in one way or another contributed to the preparation and completion of this study and provided invaluable assistance and whom I would be happy to support to express my gratitude:

I would like to thank both the German Federal Ministry of Education and Research (BMBF) and the West African Science Service Centre on Climate Change and Adapted Land use (WASCAL) for the scholarship. It has been an honour for me to be among the first recipients of this grant on the future topic of green hydrogen in West Africa. I am indebted to them for providing me with complete academic freedom to carry out this research.

I am incredibly grateful to the President of Abdou Moumouni University and the Dean of the Faculty of Science and Techniques for making it possible to hold these Master's courses on the premises of their institution and for awarding me a Master's degree in Energy and Green Hydrogen Technology.

I would also like to offer my special thanks to the Management Staff of the research centre Forschungszentrum Jülich GmbH for providing me with a research opportunity at their Institute for Energy and Climate Research (IEK) / Energy Systems Engineering (IEK-10) to complete my Master's thesis.

I would like to express my sincere gratitude to my thesis supervisors: Prof. Dr.-Ing. Andrea Benigni from Forschungszentrum Jülich GmbH, Ass. Prof. Mounkaila Saley Moussa and Dr. Souley Kallo Moutari, both from Abdou Moumouni University. Their invaluable advice and guidance were instrumental in the completion of this work.

I feel a deep sense of gratitude towards Prof. Adamou Rabani, Director of WASCAL DRP CCE. He has been a continuous source of inspiration for me, and his immense knowledge and extensive experience have been a great encouragement throughout my academic research and daily life.

My thanks to the Coordinator and Deputy Director of WASCAL DRP-CCE, Ass. Prof. Inoussa Maman Maarouhi, the Scientific Coordinator, Ass. Prof. Mounkaila Saley Moussa, as

well as Dr. Ayouba Mahamane Abdoulkadri, Coordinator of the IMP-EGH Programme, WASCAL DRP-CCE. I am grateful for all your generosity, your assistance and support, and your efforts in making my life in Niamey as enjoyable as possible.

It is also my pleasure to acknowledge the tremendous contribution made by my advisors Pan Yiwen, Li Chuan and Giacomo Tartari from the research centre Forschungszentrum Jülich GmbH, throughout all stages of the research project.

Last but not least, I want to express my sincere gratitude to the founder of First Love Church International as well as the pastors of First Love Church Cape Coast and First Love Church Niamey. Meeting you through this study program was a blessing. I appreciate your extraordinary work in motivating me and guiding me toward God's principles.

All the best to you and may God bless you all.

Abstract

Global population growth and industrialization have led to a rise in greenhouse gas emissions, particularly in the transport sector. Decarbonizing transport modes using green hydrogen fuels can help address energy transition, climate change mitigation, and sustainable development. However, the high cost of producing green hydrogen is a factor limiting the development of hydrogen-based renewable initiatives. Therefore, sizing green hydrogen refuelling stations through optimization is crucial to balancing renewable energy production, hydrogen production and storage capacity, and ultimately reducing the cost of green hydrogen production. In this context, this study aims to analyse three different technical solutions that can be developed and implemented to produce green hydrogen for refuelling stations using solar and wind energy. The study focused on the sub-prefecture of Baté-Nafadji in Guinea, known for its significant photovoltaic potential, and yielded promising results. Three hybrid renewable power generation systems, namely a hybrid PV-wind and battery system, a grid-connected PV system, and a stand-alone PV and battery system are proposed and analysed. The analysis is performed using the open-source framework COMANDO for energy systems optimization. The economic analysis has shown that the three hydrogen production configurations are economically viable for the site under consideration compared to the renewable-powered hydrogen refuelling stations described in the literature. The optimized solution shows that a grid-connected PV hydrogen refuelling station with a capacity of 7.2 MW can generate 87,600 kg of green hydrogen annually, with a levelized cost of hydrogen of 2.67 $/kg and a total net present cost of 47,541,000 $. This research will benefit policy-makers, energy planners and investors concerned with Guinea's transition to sustainable transportation solutions.

Keywords: Optimal sizing, Green hydrogen, Refuelling stations, Hydrogen vehicles, Sustainable transport.

Résumé

La croissance de la population mondiale et l'industrialisation ont entraîné une augmentation des émissions de gaz à effet de serre, en particulier dans le secteur des transports. La décarbonisation des modes de transport à l'aide de carburants à base d'hydrogène vert peut contribuer à la transition énergétique, à l'atténuation du changement climatique et au développement durable. Toutefois, le coût élevé de la production d'hydrogène vert est un facteur qui limite le développement d'initiatives en matière d'énergies renouvelables basées sur l'hydrogène. Par conséquent, le dimensionnement des stations de ravitaillement en hydrogène vert par optimisation est crucial pour équilibrer la production d'énergie renouvelable, la production d'hydrogène et la capacité de stockage, et finalement réduire le coût de la production d'hydrogène vert. Dans cette optique, cette étude vise à analyser trois solutions techniques différentes qui peuvent être développées et mises en œuvre pour produire de l'hydrogène vert pour les stations de ravitaillement en utilisant l'énergie solaire et l'énergie éolienne. L'étude s'est concentrée sur la sous-préfecture de Baté-Nafadji en Guinée, connue pour son important potentiel photovoltaïque, et a donné des résultats prometteurs. Trois systèmes hybrides de production d'énergie renouvelable, à savoir un système hybride solaire-éolien avec batterie, un système solaire connecté au réseau et un système solaire et autonome avec batterie, sont proposés et analysés. L'analyse est réalisée à l'aide du logiciel gratuit COMANDO qui permet d'optimiser les systèmes énergétiques. Les résultats de l'analyse économique ont montré que les trois configurations de production d'hydrogène sont économiquement viables pour le site considéré par rapport aux stations de ravitaillement en hydrogène alimentées par des sources d'énergie renouvelables décrites dans la littérature. La solution optimisée montre qu'une station de ravitaillement en hydrogène alimentée par un système photovoltaïque connecté au réseau et d'une capacité de 7,2 MW peut générer 87 600 kg d'hydrogène vert par an, avec un coût actualisé de 2,67 $/kg et une valeur actuelle nette de 47 541 000 $. Cette recherche profitera aux décideurs politiques, aux planificateurs énergétiques et aux investisseurs concernés par la transition de la Guinée vers des solutions de transport durables.

Mots clés : Dimensionnement optimal, Hydrogène vert, Stations de ravitaillement, Véhicules à hydrogène, Transport durable.

Acronyms and abbreviations

AC	Alternative Current
AEO	African Economic Outlook
AGER	Guinean Agency for Rural Electrification
AMLs	Algebraic Modelling Languages
BEVs	Battery Electric Vehicles
BMBF	Federal Ministry of Education and Research
BSD	Strategy and Development Office /Guinea
CAPEX	Capital Expenditures
CC	Climate Change
CCS	Carbon Capture and Storage
CO_2	Carbon Dioxide
COP	Coefficient of Performance
CRF	Capital Recovery Factor
DC	Direct Current
DNE	National Directorate of Energy / Guinea
DOD	Depth of Discharge
DRP-CCE	Doctoral Research Programme in Climate Change and Energy
EDG	Electricité de Guinée (Electricity of Guinée)
FCEVs	Fuel Cell Electric Vehicles
GDP	Gross Domestic Product
GHGs	Greenhouse Gas
GHI	Global Horizontal Irradiance
GHRS	Green Hydrogen Refuelling Stations
GMT	Greenwich Mean Time
GNF	Guinean Franc
GTIopta	Global Tilted Irradiation at Optimum Angle
H_2	Dihydrogen
HFCVs	Hydrogen Fuel Cell Vehicles
HRS	Hydrogen Refuelling Stations
ICEVs	Internal Combustion Engine Vehicles
IEA	International Energy Agency
IEK	Institute of Energy and Climate Research

IEK-10	Institute of Energy Systems Engineering
IMP-EGH	International Master Program in Energy and Green Hydrogen
ITA	International Trade Administration
LCA	Life Cycle Assessment
LCOH	Levelized Cost of Hydrogen
LDVs	Light-Duty Vehicles
NGOs	Non-Governmental Organisations
NPC	Net Present Cost
NREL	National Renewable Energy Laboratory
PCU	Pre-Cooling Unit
PEM	Proton Exchange Membrane
PERD	Decentralized Rural Electrification Project / Guinea
PHEVs	Plug-In Hybrid Electric Vehicles
PLDVs	Passenger Light-Duty Vehicles
PV	Photovoltaic
SIE	Système d'Information Energétique / Guinea
UTC	Coordinated Universal Time
WASCAL	West African Science Service Centre on Climate Change and Adapted Land use
WTO	World Trade Organization

List of tables

List of figures

Table of Contents

1. Introduction

1.1. Background and motivation

Global concerns about the impact of climate change (CC) on our planet, the depletion of finite fossil fuel reserves, and the imperative to transition toward sustainable and eco-friendly energy solutions are becoming increasingly pressing (Höök & Tang, 2013, Alsayegh, 2021 and Yohannes & Diedou, 2022). The transport sector is one of the most challenging sectors to decarbonize and contributes significantly to air pollution and carbon dioxide (CO_2) emissions due to its heavy reliance on burning fossil fuels. This makes it one of the key sectors in terms of energy transition. According to the International Energy Agency (IEA), transport has the highest reliance on fossil fuels of any sector, making electric vehicles crucial for reducing emissions and harmful air pollution in cities, as well as for reducing countries' dependence on oil imports. Population growth, increasing industrialization and continued heavy dependence on fossil fuels have led to a significant rise in global CO_2 emissions, despite major technology-driven improvements in energy efficiency and the rapid growth of renewables for power generation (Barhoumi et al., 2022). Over the coming decades, demand for transportation is expected to rise as the world's population expands, incomes rise, and more people can afford cars, trains, and aeroplanes (Ritchie, 2020). Global transport will double, car ownership rates will increase by 60%, and the demand for air passenger and freight transport will triple by 2070 (IEA, 2020). Combined, all these factors would lead to a sharp rise in transport emissions, making transport crucial to achieving broader decarbonization targets. In this context, hydrogen, especially when produced through electrolysis powered by renewable energy sources, has shown promise as an alternative to traditional fossil fuels, offering a clean and versatile energy carrier with the potential to revolutionize the transport industry. Hydrogen fuel cell vehicles (HFCVs) have emerged as an alternative to conventional internal combustion engine vehicles (ICEVs), offering zero-emission mobility with the potential for long-range travel and rapid refuelling (Contestabile et al., 2011 and Apostolou & Xydis, 2019). However, the environmental benefits of HFCVs are only maximized if the hydrogen they use is produced from renewable sources and the carbon emissions associated with traditional hydrogen production methods are avoided.

Despite the fact that green hydrogen has many potential advantages, it is crucial to address the challenges with its production, storage, and fuelling, including the deployment of infrastructure to support hydrogen vehicles. Optimal sizing parameters for such refuelling

stations are not fully determined in a systematic manner. It is common for existing studies to ignore the optimization of the overall system by focusing on only one aspect, such as renewable energy sizing or station design. The optimization process involves a complex interplay of factors, including renewable energy sources, hydrogen demand, storage technology, and station components. It provides insights into cost-effective and efficient operation by optimizing each component's size. To fully benefit from the potential of green hydrogen as a clean transport fuel, and to guide the implementation of a hydrogen refuelling infrastructure, this gap needs to be addressed. This research will benefit policy-makers, energy planners and investors concerned with Guinea's transition to sustainable transportation solutions. This study's outcomes will inform decision-making for sustainable transportation in Guinea by offering insights into green hydrogen refuelling infrastructure's technical, economic, and environmental dimensions.

In the following sections of this document, we will discuss the statement of the research problem, the research questions, the research objectives as well as the research hypotheses. And this introductory part will end with the announcement of the main points of the document.

1.2. Problem statement

The global transportation sector is a major contributor to greenhouse gas (GHGs) emissions and air pollution and requires a transition to cleaner and more sustainable fuel alternatives. To accelerate the global transition to zero-carbon transport, there are a growing number of regulatory measures, including the upcoming ban on the sale of internal combustion engine vehicles (ICEVs), and ongoing improvements in technology (Conzade et al., 2022). Consequently, the future of the car is becoming increasingly electric all over the world. The world's major automotive markets are expected to sell only electric vehicles by 2035, and 80% of global vehicle sales will be electric by 2050 (Conzade et al., 2022). Pushing for more sustainable mobility means promoting the use of electric vehicles, which include battery electric vehicles (BEVs), plug-in hybrid electric vehicles (PHEVs) and fuel cell electric vehicles (FCEVs). To promote the use of FCEVs, which offer many advantages over others, it is crucial to build the necessary facilities to meet this need in the near future, including GHRS powered by renewable energy production systems (Gökçek & Kale, 2018a). Hydrogen refuelling stations (HRS) are a key infrastructure for the successful deployment of hydrogen-powered mobility (Caponi et al., 2021a).

Guinea is a country rich in renewable energy resources that could show interest in adopting hydrogen as a clean fuel for its transportation sector. The country's abundant

renewable resources, such as solar and wind energy can be harnessed by establishing GHRS. However, the economics of green hydrogen are challenging, mainly because the underlying costs and availability of renewable energy sources vary considerably (PwC, n.d.). The high cost of producing green hydrogen today is a limiting factor to the development of hydrogen-based renewable energy initiatives, and therefore an obstacle to the large-scale deployment of HFCVs. The development of efficient GHRS is highly desirable to reduce the cost of producing green hydrogen and therefore the life cycle cost of HFCVs (Xu et al., 2022). This study aims to contribute to Guinea's efforts to adopt cleaner transportation solutions and mitigate the impacts of climate change by providing valuable insights into the design and implementation of GHRS.

1.3. Research questions

This master's thesis aims to address the following key questions:

1.3.1. Central question

Considering technical, economic and environmental factors, what is the optimal solution for producing green hydrogen for refuelling stations to support the deployment of hydrogen vehicles in Guinea?

1.3.2. Sub-questions

(1) What are the optimal sizing strategies for GHRS in Guinea considering technical, economic and environmental factors?
(2) What are the potential barriers and limitations in implementing GHRS in Guinea and how can they be addressed?
(3) Is it technically and economically feasible to set up GHRS on the proposed site?

1.4. Research hypotheses

1.4.1. Main hypothesis

The optimal sizing of renewable-powered GHRS, taking into account factors like renewable energy availability, hydrogen storage capacity, and hydrogen demand, can enhance efficiency, sustainability, and economic viability, promoting hydrogen vehicle adoption in transportation.

1.4.2. Secondary hypotheses

(1) Establishing a green hydrogen infrastructure in Guinea will lead to the development of a sustainable energy sector.
(2) Integrating renewable energy sources like solar and wind into GHRS in Guinea will leverage abundant and sustainable energy resources and minimize the dependency on fossil fuels.
(3) Introducing GHRS in Guinea can greatly decrease greenhouse gas emissions in the transportation industry.

1.5. Research objectives

1.5.1. General objective

Overall, this study aims to determine the optimal sizing of GHRS powered by renewable energy sources for hydrogen vehicles in Guinea, providing insights into the technical, economic, and environmental aspects of such refuelling stations.

1.5.2. Specific objectives

(1) Thoroughly examine the literature on the design of HRS, optimization techniques, and hydrogen vehicle technology. This will provide an understanding of the field's current state and help identify areas that need to be explored further.
(2) Gather relevant data on the potential of renewable energies (solar and wind) in Guinea, as well as the technical and economic data on HRS' components.
(3) Evaluate various electrolysis technologies for green hydrogen production, taking into account efficiency, scalability, and compatibility with renewable energy sources.
(4) Develop a mathematical model or an optimization algorithm to determine the optimal sizing of the GHRS components (electrolyser capacity, storage capacity, compressor capacity, PV modules and wind turbine capacity).
(5) Conduct an economic analysis that takes into account capital costs, operational costs, maintenance expenses, and potential revenue from electricity sales, and compare the economic feasibility of different sizing scenarios.
(6) Compare the economic feasibility of different sizing scenarios and assess the potential for cost reductions over the lifetime of the HRS.
(7) Analyse the optimal sizing methods and provide recommendations for the design of a GHRS tailored to Guinea's specific needs

(8) Apply the developed sizing method to Guinea's specific context, taking into account the country's renewable energy potential, transport patterns and hydrogen demand forecasts.
(9) Highlight the study's contributions to the field of green hydrogen technology, the integration of renewable energies and sustainable transport by summarising the findings.

1.6. Outline of the document

This document is set out in five main parts which are organised as follows:

(1) The introduction part provides the overall context and justification for the study, along with background details on the issue being addressed, the research questions, hypotheses, and objectives.
(2) Chapter 1 highlights relevant literature that assesses the technical and economic feasibility of hydrogen systems and hydrogen refuelling stations.
(3) Chapter 2 provides an explanation and justification for the research methodology used by presenting the study area, explaining the data collection methods (list your data and the methods, tools or materials, and techniques used to collect them) and describing the data processing and analysis (the methods, techniques and software used for data processing and analysis).
(4) Chapter 3 presents the results and discussions. The results section presents the main findings of the data collection and analysis, while the discussion section explores the meaning, significance and relevance of the results.
(5) The last part of the document includes both the conclusion and the perspectives. The conclusion section determines the validity of the hypothesis and recaps the findings for the research questions, while the perspectives section outlines how the study will be enhanced or expanded in the future.

2. Chapter 1: Literature review

2.1. Introduction

As governments and corporations increasingly commit to tackling CC and reducing emissions, they are placing greater emphasis on the in-depth decarbonization of hard-to-abate energy-intensive sectors such as transport (De Blasio, 2021). The transport of goods and people is one of the main causes of the increase in global GHGs emissions since preindustrial times. This substantial contribution to GHGs emissions has made the transport sector an increasingly important area of study and concern. Various studies have been carried out to demonstrate how GHRS powered by renewable energies are crucial in the transition towards sustainable, low-carbon transport, and how their optimal sizing can facilitate the expansion of the network of such infrastructures worldwide. This review of the literature surveys previous research on the importance of HRS for sustainable transportation and on the importance of optimal sizing of renewable-powered GHRS. It provides a comprehensive understanding of the current state of the field and identifies areas for future research.

2.2. Alternatives to fossil fuels in transport

Among the many alternative fuels available today, hydrogen can be seen as an interesting solution for replacing current carbon-based fuels. The net-zero ambition can be achieved by decarbonising transport modes using green hydrogen-fuelled alternatives, hydrogen generated through electrolysis using renewable energy sources such as solar and wind power (ARUP, n.d.). Hydrogen is the lightest of all gases and a versatile, clean, and flexible energy carrier that can be produced from diverse domestic resources and used in many applications. Hydrogen fuel has the highest energy content by weight of any known conventional fuel. Its energy content per mass is almost three times that of gasoline (U.S. Department of Energy, 2019). Depending on the energy source and production method used to produce hydrogen, there are various types of hydrogen distinguished by colour. The main types of hydrogen under consideration are grey hydrogen, blue hydrogen, and green hydrogen (Pascal, 2022):

- **Grey hydrogen:** The most commonly used type of hydrogen is grey hydrogen, which is produced through a process known as "steam reforming" using natural gas or methane.

- **Blue hydrogen:** When the carbon produced by steam reforming is captured and stored underground using industrial carbon capture and storage (CCS), the hydrogen is designated as blue.
- **Green hydrogen:** Green hydrogen, also known as clean hydrogen, is generated by using renewable energy sources like solar or wind power. Through a process called electrolysis, water is split into two hydrogen atoms and one oxygen atom.
- In the energy industry, other colours such as black, brown, red, pink, yellow, turquoise and white are used for molecular hydrogen.

Hydrogen is increasingly being discussed as a promising fuel that could reduce the amount of fossil fuels consumed in various sectors such as transportation and heavy industry, and help to reach the net-zero emissions targets by 2050 (Ewing et al., 2020). As it can reduce carbon dioxide emissions, reduce dependence on fossil fuels and improve the economics of the energy sector, green hydrogen is required for environmentally friendly transport and many other industrial applications (Barhoumi et al., 2022). Hydrogen and FCEVs are frequently mentioned as key components in the decarbonization of transport systems (Ajanovic & Haas, 2021). FCEVs are essentially pure electric vehicles in which chemical energy is stored as compressed hydrogen, typically in 35 or 70 MPa high-pressure tanks (Micena et al., 2020). Hydrogen stores energy, flows into a fuel cell, reacts with oxygen from the air, and creates electricity that powers the electric motor. The development of electric vehicles, including FCEVs, offers a viable solution for reducing emissions from passenger vehicles as the world moves towards lower-carbon sources of electricity (Ritchie, 2020). In its Global Hydrogen Review 2021, the IEA reported that by the end of June 2021, there were more than 40,000 FCEVs in circulation worldwide. The global deployment of FCEVs has been largely concentrated on passenger light-duty vehicles (PLDVs), accounting for 74% of FCEVs registered in 2020 (IEA, 2021b). The main advantages of this type of vehicle are that they offer greater autonomy and less dependence on the battery, and that, unlike traditional electric vehicles, their refuelling times are similar to those of internal combustion vehicles (Apostolou & Xydis, 2019). But, transitioning to hydrogen-powered mobility requires the development of an infrastructure capable of meeting the demand for hydrogen (Di Micco et al., 2022). Hydrogen refuelling stations are infrastructures dedicated to this purpose. Hydrogen refuelling stations are crucial in the transition to a hydrogen-based economy due to their ability to increase the market penetration of hydrogen vehicles (Apostolou & Xydis, 2019). Although FCEVs have been on the market for a decade, registrations are still more than two orders of magnitude lower than those of

PHEVs. This is partly because HRS are not widely available and unlike plug-in electric vehicles, FCEVs cannot be recharged at home (IEA, 2021a). Without an extensive network of hydrogen refuelling infrastructures, hydrogen vehicles are strongly limited in terms of operation and their commercial deployment will be very limited (Caponi et al., 2021b). According to The Global Electric Vehicles Outlook of the IEA (IEA, 2022), there were about 730 HRS worldwide supplying fuel for about 51 600 FCEVs in 2021, representing an increase of almost 50% in the global FCEVs stock and a 35% increase in the number of HRS from 2020. And over 80% of FCEVs on the road at the end of 2021 were light-duty vehicles (LDVs), with the majority being passenger cars. Buses and trucks each account for almost 10% of the global FCEV fleet.

2.3. Renewable-powered GHRS

HRS is a facility that dispenses hydrogen at a pressure of 350 and 700 bar (H35 and H70) to supply FCEVs (HYDEVA, n.d.). There are basically two types of HRS based on the hydrogen supply method (Micena et al., 2020):

- **Off-site HRS:** In the off-site type of HRS, hydrogen is produced in an off-site industrial facility outside the site of the hydrogen station, from which it is transported to the hydrogen station via pipeline, highway, railroad or ship. Hydrogen is received at low pressure and it must be compressed and cooled before it can be transferred to the vehicle tank.
- **On-site HRS:** In the on-site type of HRS, hydrogen is produced locally from energy sources available at the plant site, whether renewable or not, such as solar, wind, biomass or fossil fuels.

This study will focus on the on-site HRS that produces hydrogen from the electrolysis of water using renewable energy sources. The electrolysis of water using renewable energy, also known as green hydrogen, is an attractive approach for producing hydrogen with low carbon emissions (Hussain et al., 2022). On-site HRS are best suited for remote areas with low demand, while off-site HRS are more suitable for urban areas with high demand (Stars & Qin, 2014). The on-site HRS are an interesting solution for assuring green hydrogen with zero CO_2 emissions. The advantages of this solution are (Di Micco et al., 2022): i) increasing of the share of electricity generated from renewable sources, ii) assisting the integration of fluctuating and non-predictable renewable energies (solar and wind) into the electricity grid, iii) the provision of grid balancing services, iv) and producing green hydrogen that can ensure sustainable transportation. A regular on-site HRS consists of renewable energy sources, electrolysers, hydrogen gas compressors, hydrogen storage tanks and a hydrogen dispenser, which can

dispense hydrogen at 350 bar, 700 bar, or dual pressures, depending on the type of vehicle being refuelled (Micena et al., 2020).

The increasing interest in hydrogen-powered vehicles as an alternative to traditional fossil fuel-based transportation highlights the importance of the availability and accessibility of hydrogen refuelling infrastructure for their widespread adoption. The study conducted by Apostolou & Xydis, 2019 presented a comprehensive evaluation of current HRS technologies, including station components and categories, to showcase the promising potential of the emerging hydrogen road transport market. It was concluded that HRS and FCEVs have a symbiotic relationship, meaning that investing in HRS will yield significant returns only if there are more FCEVs, but suboptimal development of the hydrogen infrastructure will impede the growth of this market. Overall, to benefit from the advantages of those FCEVs, safe and reliable HRS are needed. HRS are crucial in the transition to a hydrogen-based economy due to their ability to increase the market penetration of hydrogen vehicles (Apostolou & Xydis, 2019).

2.4. Optimal sizing of HRS

The optimal sizing of renewables-powered GHRS is crucial for the successful integration and growth of hydrogen vehicles in the transport sector. Various research studies have been conducted regarding the optimal sizing of renewables-powered GHRS to ensure their efficiency and cost-effectiveness, scalability and future growth, environmental benefits, economic viability, integration of renewables and reliability of hydrogen supply. For instance, Ayodele et al., 2021 conducted a techno-economic evaluation of a wind-powered HRS in seven cities in South Africa, intending to determine the optimal configuration of an HRS powered by wind energy resources for each of the cities, as well as to determine their economic viability and carbon reduction capacity. The results showed that a wind-powered HRS is viable in South Africa with the cost of hydrogen production ranging from 6.34 $/kg to 8.97 $/kg. Similarly, Hussain et al., 2022 proposed a model for the optimal sizing of the key components of a renewable hydrogen production and fuelling station. Simulation results provided using the available cost parameters in the context of the Canadian market show that a GHRS powered only by wind and solar power could produce hydrogen at less than 6.8 $/kg when financing costs are taken into account, or up less than 5 $/kg if financing costs are neglected. Furthermore, to determine the optimum solutions for the production of green hydrogen, Barhoumi, Okonkwo, Ben Belgacem, et al., 2022 carried out the optimal sizing of GHRS based on photovoltaic systems in Oman. The economic analysis showed that for the site under consideration, the HRS

powered by the grid-connected photovoltaic system represents a promising green hydrogen production method, and allows to generate 58,615 kg of green hydrogen per year at a levelized cost of 5.5 $/kg and a total net present cost of 4,169,200 $.

Gökçek & Kale, 2018b analysed the cost of producing hydrogen using local energy resources in an HRS in Turkey. They employed a hybrid wind PV power system and found it to be economically viable. The levelized cost of hydrogen production varied between 7.526 and 7.866 $/kg depending on the system configuration. Another study by Gökçek & Kale, 2018a conducted a comprehensive techno-economic analysis to determine the viability of an HRS running on hybrid renewable energy systems. The study calculated the levelized cost of hydrogen under varying parameters such as wind speed, hub height, solar irradiance, project lifetime, and additional components. The research findings indicated the feasibility of the HRS powered by hybrid renewable energy production systems for the selected location.

For on-site HRS that purchase power from the electricity market to produce hydrogen, the operational costs of the facility are highly dependent on electricity prices. For instance, Dadkhah et al., 2021 assessed the feasibility of such an HRS and revealed that operational costs are extremely dependent on electricity price and grid costs, directly associated with the electrolyser's size. Therefore, optimizing component sizing and considering exemptions from taxes or other grid-related costs are essential for achieving economic viability.

When setting up an HRS, both techno-economic analysis and optimal sizing of the sub-components are crucial. Kavadias et al., 2022 investigated the effect of the number of vehicles that the facility can refuel to balance initial investment cost and fuel cost in remote areas. They conducted equipment sizing and financial analysis of a GHRS powered by surplus electrical energy from a wind farm. The results highlighted the viability of appropriately sized wind-powered HRS and the potential for hydrogen to store rejected wind energy. Additionally, scenarios with low hydrogen vehicle penetrations exhibited lower economic performance due to significant increases in payback periods. In the same way, Micena et al., 2020 proposed a comprehensive methodology for sizing the components of an on-site HRS powered by a photovoltaic plant. This methodology included calculating hydrogen vehicle demand, main component parameters, refuelling station energy consumption, and solar photovoltaic plant power. The conclusion drawn was that hydrogen production costs are inversely proportional to the production capacity of an HRS; costs increased notably for stations with lower demand.

To summarize, the literature reviews presented a comprehensive exploration of the optimal sizing of GHRS powered by renewable energy. This would help promote the adoption and growth of hydrogen vehicles in the transportation industry. The studies highlighted the crucial need to ensure efficiency, affordability, scalability, environmental advantages, economic feasibility, renewable integration, and hydrogen supply reliability.

2.5. Gaps and contributions

The purpose of a literature review is not only to understand what has already been accomplished in previous research but also to pinpoint any gaps that require further exploration in new studies. This section aims to state the gaps in the literature regarding the topic being studied. The literature reviewed for this study revealed a few gaps that we intend to fill in this study:

(1) Existing studies often neglect the optimization of the overall system by only focusing on one aspect, such as renewable energy sizing or station design. This study aims to develop a comprehensive optimization model that considers various parameters, such as renewable energy source availability, hydrogen demand, storage technologies, and station components. This model could provide insights into the optimal sizing of each component for cost-effective and efficient operation.

(2) Numerous optimization studies rely on specific problem classes, such as linear programming or mixed-integer linear programming. Energy system models may also impose restrictions to stay within these classes. However, this method does not provide enough detail for technical system design and operation. In this study, the flexible open-source framework COMANDO, which does not impose restrictions to maintain the optimization problems in a particular class is used. COMANDO combines desirable functions of existing tools and offers levels of abstraction suitable for structured model generation and flexible problem formulation (Langiu et al., 2021).

(3) After reviewing the literature, it appears that there is a lack of research regarding the optimal sizing of green hydrogen refuelling stations for an African case study. The green hydrogen refuelling station is a new technology in Guinea. The purpose of this study is to assess the practicality of this technology for the country and the continent of Africa as a whole.

3. Chapter 2: Methodology

The refuelling station produces green hydrogen through water electrolysis powered by renewable energy sources like solar or wind. As stated earlier, this study aims to determine the most efficient and effective configuration for hydrogen refuelling stations (HRS) that produce green hydrogen using solar and wind energy. In this chapter, we first introduce the study area and give an overview of the system itself (HRS). Next, we outline the analysis approach, identify the possible location of the HRS and explain the methods used to collect the data required for the study. Finally, we explain the techniques and software used to process and analyse the data and acknowledge the limitations of the research methodology.

3.1. Study area

The study area is located in Baté-Nafadji, a sub-prefecture in the Kankan Prefecture in the Kankan Region of eastern Guinea, between 10.721002° latitude north and 9.362760° longitude west (Encyclopaedia Britannica). The time zone is UTC+00, Africa/Conakry [GMT], with a terrain elevation of 368 m (Global Solar Atlas). In this part of the study, we explore Guinea's geography, economic context, energy, industry and transport sectors, highlighting the Baté-Nafadji sub-prefecture as a case study location.

3.1.1. Geographical context

Located in West Africa, the Republic of Guinea, literally called Guinea-Conakry, achieved national independence in 1958 and is a coastal country with around 300 km of Atlantic coastline. It covers an area of 245,857 km^2 and has an estimated population of 13.53 million in 2022 (World Bank). The country extends over 800 km from east to west and 550 km from north to south. It is bordered to the north by Senegal, to the northeast by Mali, to the northwest by Guinea-Bissau, to the southeast by Côte d'Ivoire, and to the south by Sierra Leone and Liberia. Guinea is made up of four geographical regions, to which correspond four types of topography, climate, fauna, flora, and distinct historical and cultural traditions:

(1) The coastal maritime region or Lower Guinea, of which the capital Conakry is a part, is filled with mangroves and alluvial plains where palm trees grow. Rainfall is abundant and Conakry is one of the wettest cities in the world. This region is the windiest area of the country because of its proximity to the ocean.

(2) The Futa Jallon or Middle Guinea. The Niger, Senegal and Gambia rivers originate in Futa Jallon. Many other rivers and waterfalls flow through the region's rocky escarpments and narrow valleys.
(3) To the east of Futa Jallon lies Upper Guinea, of which the city of Kankan is a part, a savannah region with plains and river valleys. Kankan is sometimes regarded as the country's second-largest city. This region is the sunniest part of the country because of its proximity to the Saharan region.
(4) The southernmost region is the forest region or Forest Guinea. Rainfall is heavy and the region is covered with rainforests of mahogany, teak and ebony.

There are significant hydrographic resources and rich mining potential in the country (75% of global reserves), gold, diamonds, high-quality iron (Simandou blocks), manganese, zinc, cobalt, nickel, and uranium reserves (Guinée Politique, 2021). NGOs that focus on water have conducted studies that show Guinea has abundant water resources, including rainwater, surface water, and groundwater. There are approximately 226 billion m^3 of renewable water resources available in 23 river basins, 14 of which are shared with neighbouring countries in the West African sub-region. Groundwater is estimated at around 13 billion m^3 (Médiaterre, 2013).

3.1.2. Economic context

Torn between economic development and environmental preservation, Guinea's national economy is mainly driven by the agricultural sector (which employs 80% of the population) and mining (bauxite, diamonds, gold, iron) (Guinée Politique, 2021). Despite its natural resources and abundant rainfall, the country remains one of the poorest in the world, with a very fragile economy dependent on bauxite and agriculture. Guinea has one-third to one-half of the world's known reserves of bauxite (the main aluminium ore), as well as significant reserves of high-grade iron ore at Mount Nimba and the Simandou Mountains (O'Toole, 2023). The Guinean GDP is driven by the production in the mining sector (26%, including the conversion of bauxite into alumina) and agriculture (20%), with the former providing 95% of export earnings and the latter the rest (WTO, 2011). The real GDP grew by around 4.8% in 2022, compared with 4.4% in 2021 (AEO, 2023).

3.1.3. Energy and industry sectors

Guinea's energy sector has enormous potential but has been underperforming for decades due to a lack of investment. The country has diverse energy resources including an

estimated 6000 MW of exploitable hydroelectric potential, a solar potential with a mean annual insolation of 4.8 kWh/m²/day, and wind potential with average annual wind speeds between 2 and 4m/s (Ministère de l'Énergie et de l'Hydraulique, 2012). Being the source of three of West Africa's main rivers (the Niger, Senegal and the Gambia), Guinea is often referred to as West Africa's water tower, due to its average annual rainfall of 2958 mm (Hammami, 2021). The country is therefore blessed with significant renewable energy resources which, through appropriate project developments, can position the country as a regional electricity producer. In order to promote green development, reduce the country's dependence on imported fuels and utilize Guinea's abundant water resources, the Guinean government has announced a long-term energy strategy with a focus on renewable energy sources such as solar and hydroelectric power. The Kaleta Dam, commissioned in 2015, is the first stage of this strategy. The 450 MW Souapiti Dam has effectively doubled the amount of electricity available (ITA, 2022). Distribution and transmission remain a challenge, but if solved, Guinea could be able to export electricity to neighbouring countries, which is the government's plan.

Apart from the mining sector, the main industries in Guinea are the food industries, the textile industries, the wood industry, the manufacture of alumina and the cement works.

3.1.4. The institutional framework of the energy sector

The organizational chart for managing the energy sector and specifically the electricity sub-sector in Guinea is illustrated in Figure 3.1 (SIE, 2023):

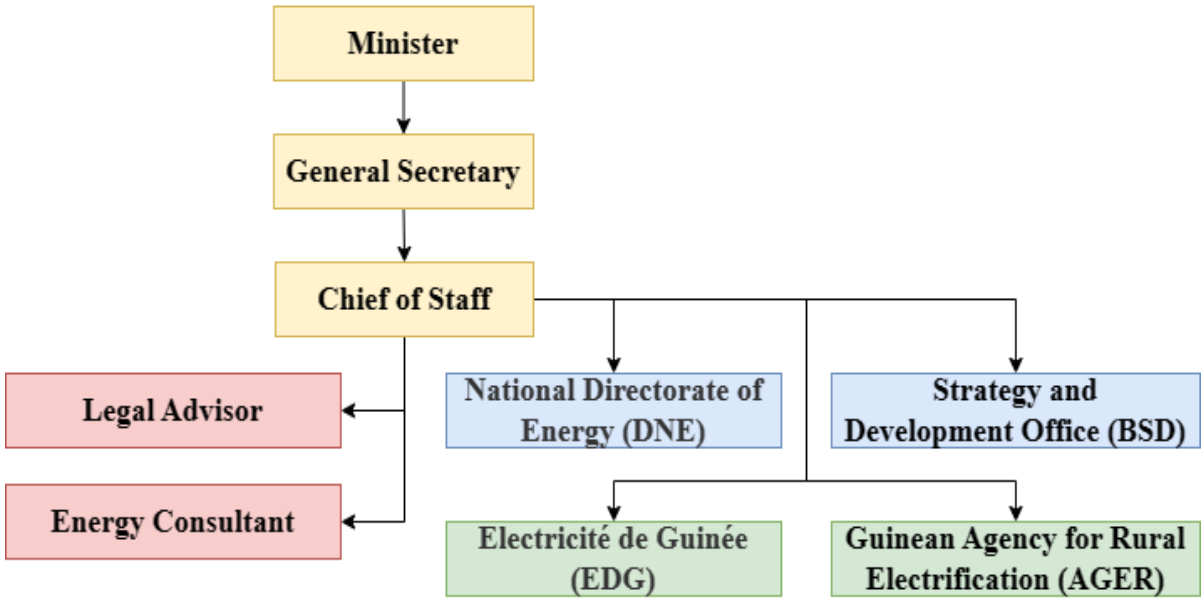

Figure 3.1: Organization chart of the Guinean Ministry of Energy

(1) **The Ministry of Energy:** Is responsible for the formulation and implementation of energy sector development policies and strategies. It exercises its powers through the following structures (National or General Directorates):

(2) **The National Directorate of Energy (DNE):**

- Development and implementation of energy strategies, policies and programs including renewable energies;
- Development and control of the application of energy regulations;
- Promotion of national energy potential (Hydropower and others).

(3) **Electricité de Guinée (EDG):** It is responsible for the public service for the production, transmission and distribution of electrical energy.

(4) **Guinean Agency for Rural Electrification (AGER):**

- Its mission is the implementation of rural electrification policy and the popularization of projects in rural areas.
- AGER is the continuation of the Decentralized Rural Electrification Project (PERD) which began in 2006 and ended in 2011 under the financing of the World Bank.

(5) **Strategy and Development Office (BSD):** Responsible for developing the development strategy for all sectors of the department.

3.1.5. Transport sector

Guinea's transportation system is largely based on roads and domestic air service. Roads connect Guinea to regional centres as well as to Senegal and Mali. An international airport in Conakry serves jets of all sizes. The Conakry-Kankan railway is now practically out of service and there is no passenger rail service in the country. Two industrial railways serve the bauxite mining areas, including a line connecting Conakry to the bauxite mines at Fria. The Boké Railway connects Kamsar with Sangaredi. The port facilities of Conakry are extensive. There is a quay with a depth of 25 to 65 feet (8 to 20 meters) and a berth with modern loading equipment. The bauxite mining company Sangaredi has its own ore export port in Kamsar (O'Toole, 2023).

3.1.6. Why Baté-Nafadji sub-prefecture as study location?

The Baté-Nafadji sub-prefecture is located on the N6 national road that links Kankan town and Siguiri town in Guinea (Figure 3.2). Kankan is the second-largest city in Guinea and serves as the commercial and transport hub of the savannah region in the northeast. Based on 2014 data, the region has a population of 1,972,537 and covers an area of 72,145 km² (Balde,

2018). Kankan region shares borders with the countries of Mali and Côte d'Ivoire, as well as with the N'Zérékoré and Faranah regions in the country.

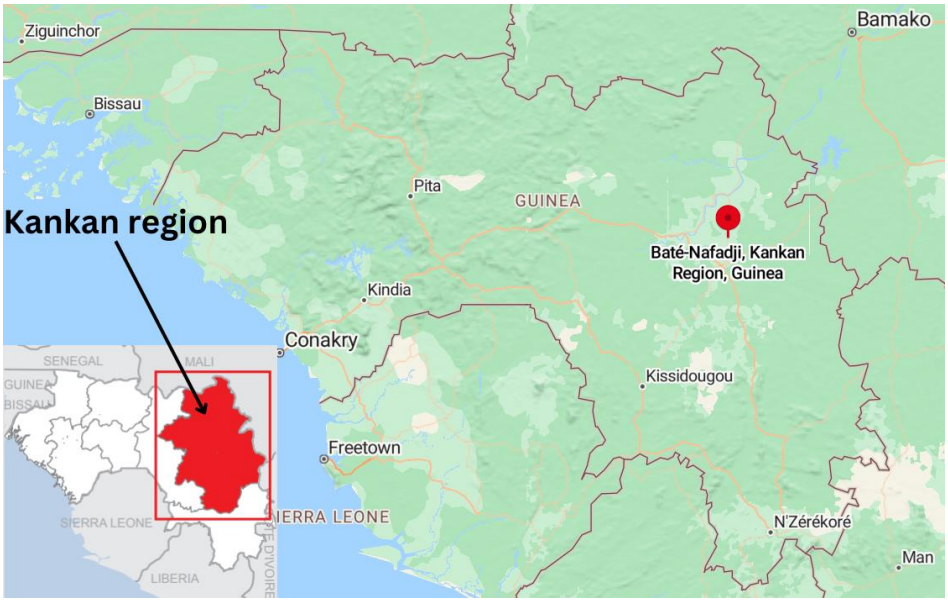

Figure 3.2: Bate-Nafadji sub-prefecture on the map of Kankan region in Guinea

Kankan is the endpoint of a 661-kilometre railway from Conakry. It serves as a central hub for routes from Bamako (Mali), Siguiri, Kouroussa, and N'Zérékoré. The Kankan region consists of 57 towns, with Kankan, Siguiri, and Kouroussa being the largest. The area's climate is primarily savannah with dry winters, and it has various light industries, including manufacturing and traditional crafts like gold, ivory, and wood (Encyclopaedia Britannica). The Kankan region receives the highest amount of sunlight annually with 2700 hours, leading to an average irradiation of 4.8 kWh/m²/day for solar energy (SYLLA, 2022). As for the wind power potential, the mean power density for the 10% windiest area in the region is 133 W/m^2 and the mean power density at a height of 100 m is 4.88 m/s (Global Wind Atlas). Therefore, the sub-prefecture of Baté-Nafadji was purposely selected, as it is well suited to achieving the research objectives and addressing the problems that motivate this study.

3.2. System description

3.2.1. System presentation

The goal of green hydrogen refuelling stations is to support sustainable transportation and reduce carbon emissions. Green hydrogen is produced by using renewable energy from solar and wind power in the electrolysis process. This makes it an eco-friendly option compared to traditional hydrogen production methods that rely on fossil fuels. The hydrogen refuelling

station system consists mainly of PV modules, wind turbines, battery storage, DC-AC converters, electrolysers, hydrogen gas compressors, hydrogen storage tanks, and a hydrogen dispensing system, as shown in Figure 3.3. This hydrogen refuelling station is designed to dispense hydrogen as a compressed gas at pressures of 700 bars (70 MPa) for light-duty fuel cell electric vehicles (passenger vehicles). The performance specifications of the hydrogen refuelling station in this study were assumed using the functional description of the station modules by (H2 Mobility, 2010). The size is assumed to be medium, with a number of refuelling positions (dispensers) of 2, and an average hydrogen throughput of 336 kg per day.

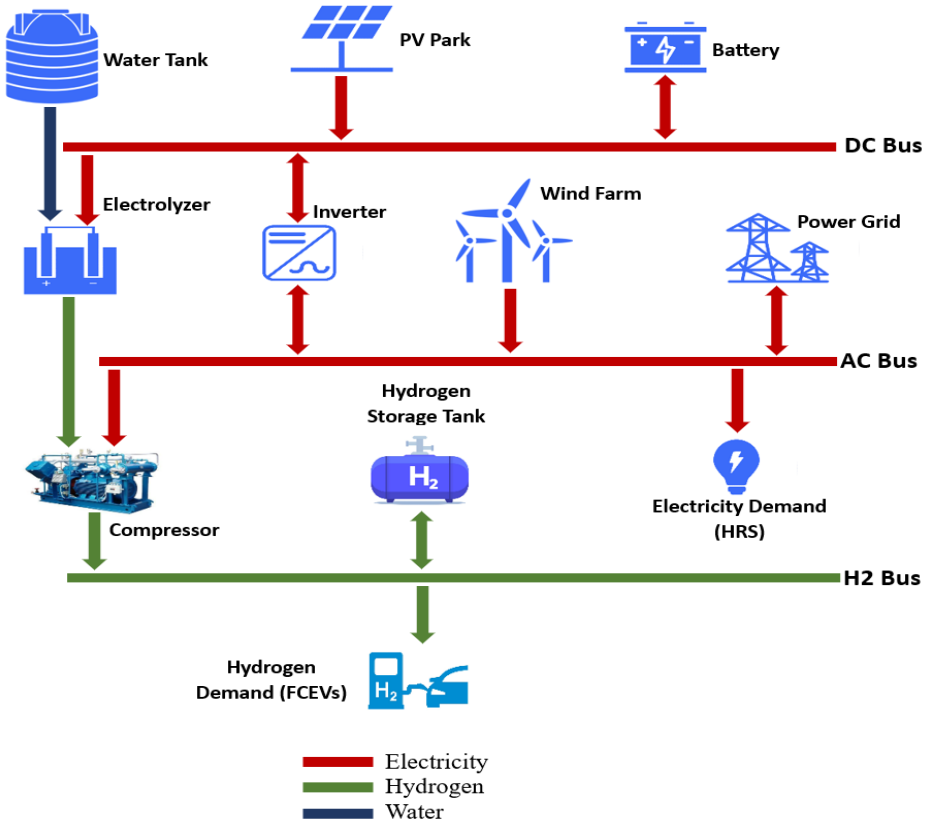

Figure 3.3: Overview of different components of the HRS system

3.2.2. System configurations

When sizing green hydrogen refuelling stations, it's crucial to determine the optimal combination of renewable energy sources, hydrogen production capacity, hydrogen storage capacity, and refuelling infrastructure. This ensures meeting the demand for hydrogen vehicles while reducing costs and negative environmental impact. In this study, three different hybrid renewable power generation systems (renewable power generation technology integrated with other power generation systems) proposed as technical solutions to produce hydrogen for refuelling stations are investigated:

(1) The first configuration is the hybrid PV-wind and battery system. In this case, the power generation system consists of photovoltaic modules, wind turbines and electric battery storage. There is no connection to the utility grid in this system. Instead, excess electricity is stored in a battery. This battery can be used to power the load when renewable energy sources don't generate enough electricity.

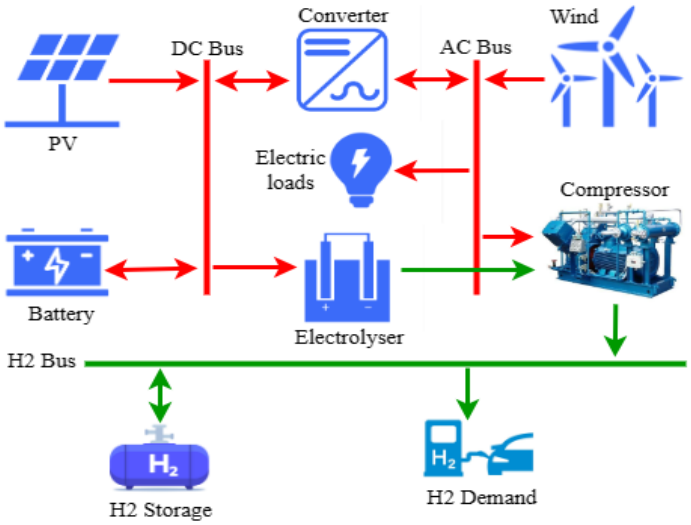

Figure 3.4: Hybrid PV-wind and battery system

(2) The second alternative solution is the grid-connected PV system. The photovoltaic modules in this system are connected to an external power grid. It is therefore possible to purchase electricity from the grid when photovoltaic production is insufficient. Surplus electricity generated by the photovoltaic modules can be sold back to the grid when it is not needed for loads.

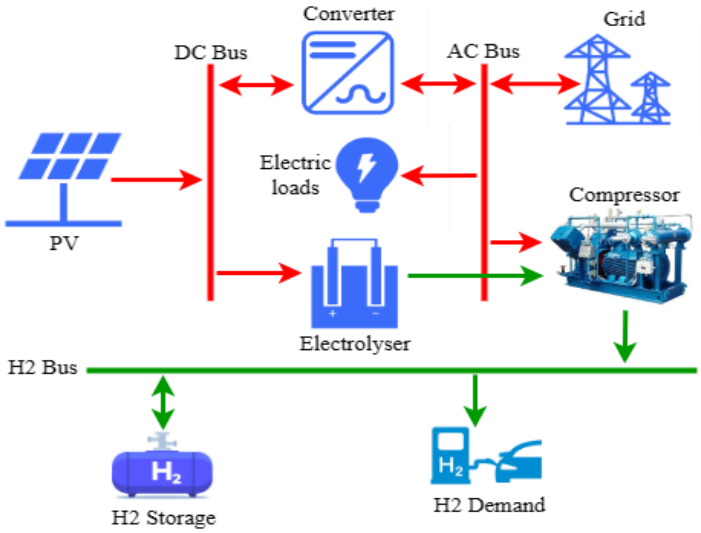

Figure 3.5: Grid-connected PV system

(3) The third and last alternative solution is the stand-alone PV and battery system. The power generation system in this case consists only of photovoltaic modules and electric battery storage. The system operates without an external power grid as well. As in the first configuration, excess electricity is stored in an electric battery, which can be tapped when the sun is not available.

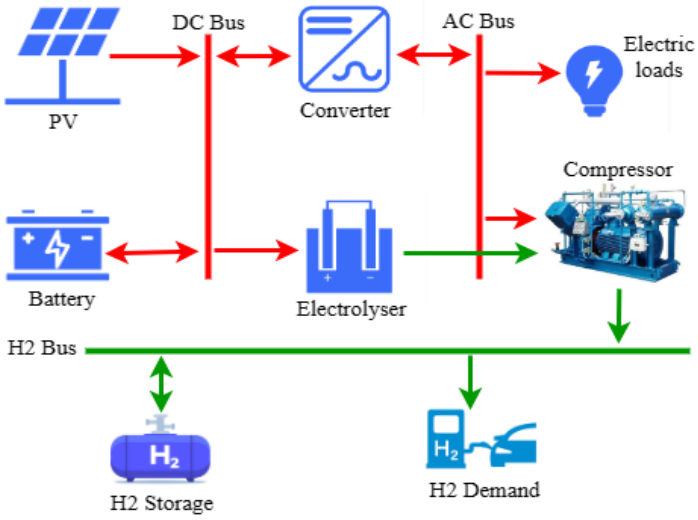

Figure 3.6: Stand-alone PV-battery system

3.3. Analysis approach

A global analytical approach was chosen to conduct this study, taking into account various factors to ensure efficiency, cost-effectiveness and environmental sustainability. The flowchart of the proposed methodology to analyse and compare different configurations of hydrogen refuelling stations is shown in Figure 3.7. First, the possible location for the hydrogen filling station was identified, taking several factors into account. This included proximity to areas where high demand for hydrogen is expected, such as cities, industries and major highways; availability of renewable energy sources (sun and wind); availability of water resources (groundwater and surface water); and land availability. After selecting the location, the required input data for the models are collected. This includes wind and solar potential, technical and economic parameters of the components, electricity sales and purchase prices, electricity demand from additional loads at the hydrogen filling station and hydrogen demand for fuel cell electric vehicles. The raw data were processed to generate usable information. Computational modelling using the open-source Python software package COMANDO has been used to analyse the green hydrogen refuelling station systems. COMANDO facilitates component-based modelling and optimisation for the non-linear design and operation of

integrated energy systems (Langiu et al., 2021). The optimisation results include optimal component sizes, infrastructure annual costs, the annual amount of hydrogen produced, and the annual amount of electricity purchased or sold in grid-connected case. To assess the cost-effectiveness of the hydrogen refuelling station with different system configurations, a techno-economic analysis was carried out by calculating the net present cost (NPC) of the project and the levelized cost of hydrogen (LCOH). This also enables a comparison of the three different system configurations. In the end, the configuration with the lowest levelized cost of hydrogen is selected.

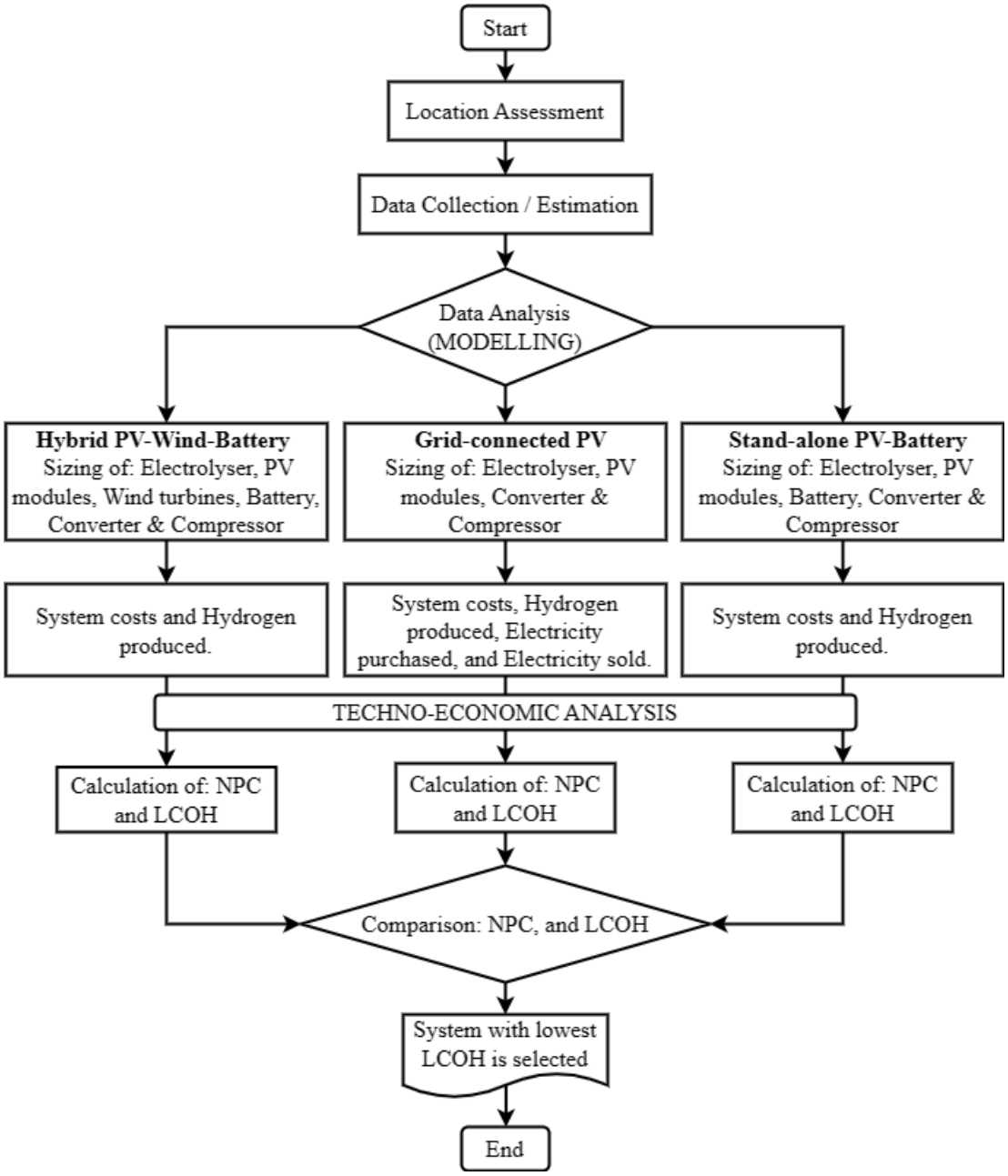

Figure 3.7: Flow chart of the analysis approach considered in this study

3.4. Data collection

In an attempt to achieve the research objectives, the following input data were collected and/or estimated: wind and solar potentials, technical and economic parameters of the different components at the hydrogen refuelling station, electricity sales and purchase prices in Guinea, electricity demand for the additional loads of the hydrogen refuelling station, and hydrogen demand for fuel cell electric vehicles.

3.4.1. Photovoltaic and wind power potential

The web tool Renewables.ninja, developed by Imperial College London and ETH Zürich, has been used to estimate the amount of energy that could be generated by wind or solar farms at the location under study. The Global Solar Altas online tool was also used to provide an overview of the region's solar energy potential. The following information about the site has been found: the global horizontal irradiance (GHI) is 2082.6 kWh/m^2, the optimal tilt of the PV modules should be 14/180° and the global tilted irradiation at the optimum angle (GTIopta) is 2134.6 kWh /m^2. In the case of wind power, the Global Wind Atlas online tool was also used to determine the availability of areas with high wind energy potential for on-site wind power generation. At 100 m altitude, the mean wind speed at the site is 4.88 m/s, while the mean wind power density, which gives a more accurate indication of the wind resource available, is 133 W/m. The average hourly photovoltaic and wind power outputs of the site are shown in Figures 3.8 and 3.9, respectively.

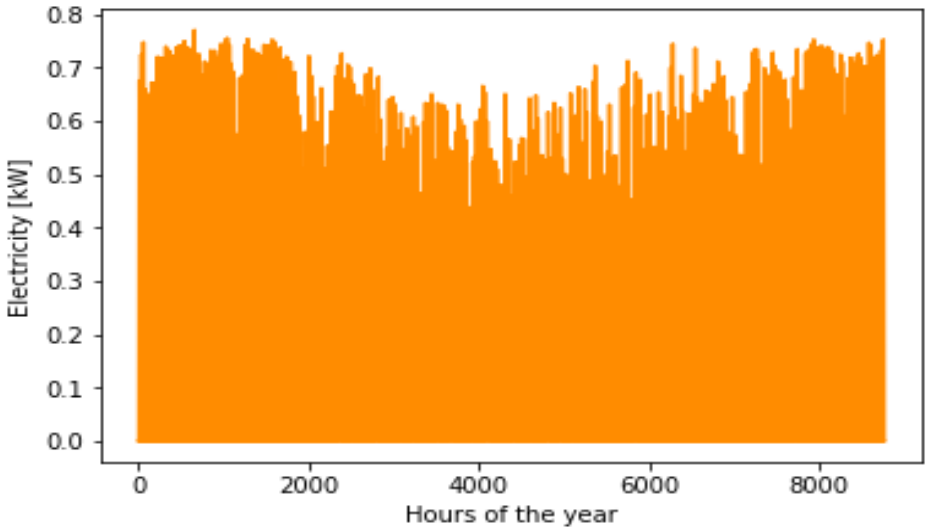

Figure 3.8: Average hourly photovoltaic power output

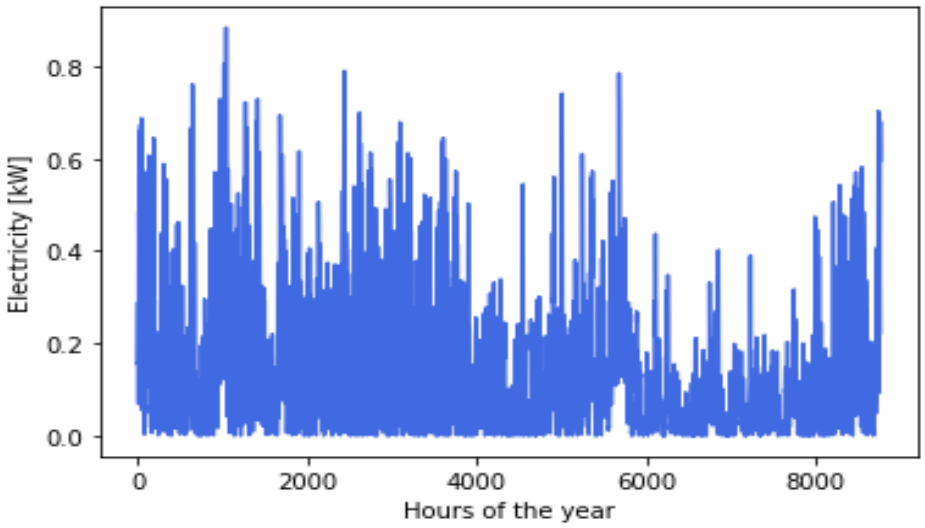

Figure 3.9: Average hourly wind power output

Clustering a full year of photovoltaic and wind data is crucial for optimization analysis in renewable energy systems. The yearly PV and wind datasets consist of long-term historical records that necessitate in-depth analysis and simulations. To address this, the lengthy historical datasets need to be condensed and clustered while maintaining the original data characteristics. The clusters that result can be used during the planning stage and in simulation studies. Therefore, for this study, the full year of the hourly photovoltaic and wind data were clustered by dividing the year into eight typical days, each consisting of 24-time steps with a duration of 1 hour per day. Each group was assigned a weight representing the number of days it included. By including the maximum and minimum irradiation days, the resulting ten representative days were used as operational scenarios in the design optimisation. The hourly PV and wind power clusters, which are used in the simulation for this study, are shown in Figures 3.10 and 3.11, respectively.

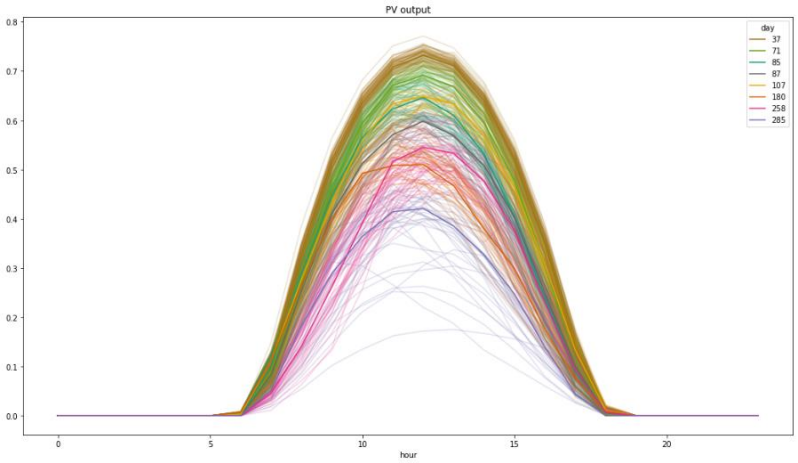

Figure 3.10: Clusters of hourly PV power output

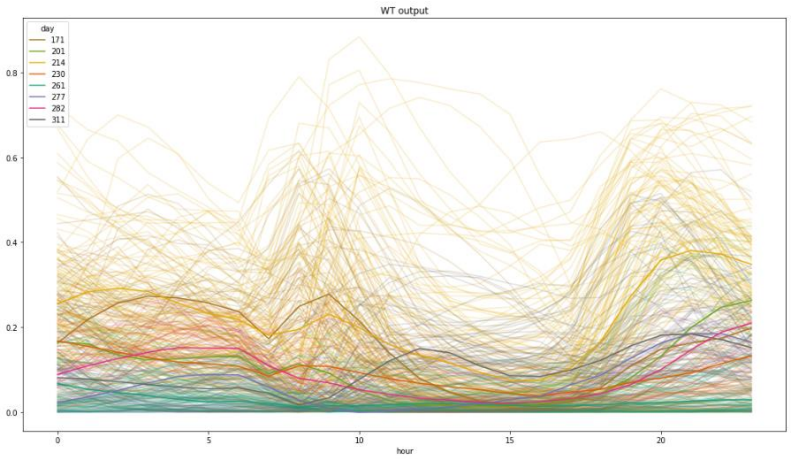

Figure 3.11: Clusters of hourly wind power output

3.4.2. Technical and economic data on components

The literature and some online open sources provided technical and financial information on the components needed to optimize each HRS system configuration. As a result, Table 3.1 lists each component's initial capital cost, annual operating and maintenance costs, replacement expenses, lifetime, and efficiency. Source: (AdeleT, 2018), (Gökçek & Kale, 2018a), (Gökçek & Kale, 2018b), (Micena et al., 2020), (Stetson & Department of Energy, 2021), (NREL, 2022) and (Urs et al., 2023).

Table 3.1: Detailed technical and economic parameters of all components

Component	Capital cost	Yearly O&M cost	Lifetime [Year]	Replacement cost	Efficiency [%]
PV modules	850 $/kW	23 $/kW	25	-	-
Wind turbines	1000 $/kW	12 $/kW	30	-	-
Converter	556.32 $/kW	1.1 $/kW	15	556.32 $/kW	95
Electrolyser	840 $/kW	2.5 %(CAPEX)	15	840 $/kW	80
Lit. ion Batterie	1087.01 $/kW	2.5 %(CAPEX)	10	925.45 $/Kw	98
Compressor	2500 $/kW	50 $/kW	25	-	70
H2 Storage tank	1448 $/kg	3 $/kg	25	-	-
Dispenser & PCU	170000 $/unit	520 $	20	170000 $	-
Water borehole	19285.5 $/unit	771.36 $	25	-	-

For this study, the project is assumed to have a duration of 25 years. Therefore, all components with a service life of 25 years or more, such as PV modules, wind turbines, compressors, hydrogen storage tanks and the borehole system, are exempt from the replacement costs.

3.4.3. Estimation of additional electricity demand

In addition to the electricity required by electrolysers and compressors, other electric loads at the hydrogen refuelling station are not considered during the optimization process but require power. The power ratings for these additional electrical loads have been obtained from the device specifications found on various commercial websites: (EnergySage, 2022), (Philips, 2023), (Radium.de, 2023), (PLEUGER, 2023). Table 3.2 shows the power ratings of these additional electrical loads.

Table 3.2: Power ratings of additional electrical loads

Device	Rated power [kW]	Quantity
Light inside	0.009	5
Light outside	0.06	4
Fridge	0.8	1
LED canopy lamp	0.095	6
Water pump	5.5	1
Office laptop	0.065	3
Fan	0.179	2
Air conditioner	5.1	2
H2 dispensing system	16.3	2

The electricity demand profile for the hydrogen refuelling station's additional electric loads was generated using Microsoft Excel 2019, after collecting their nominal power. The profile was generated on an hourly basis (Figure 3.12).

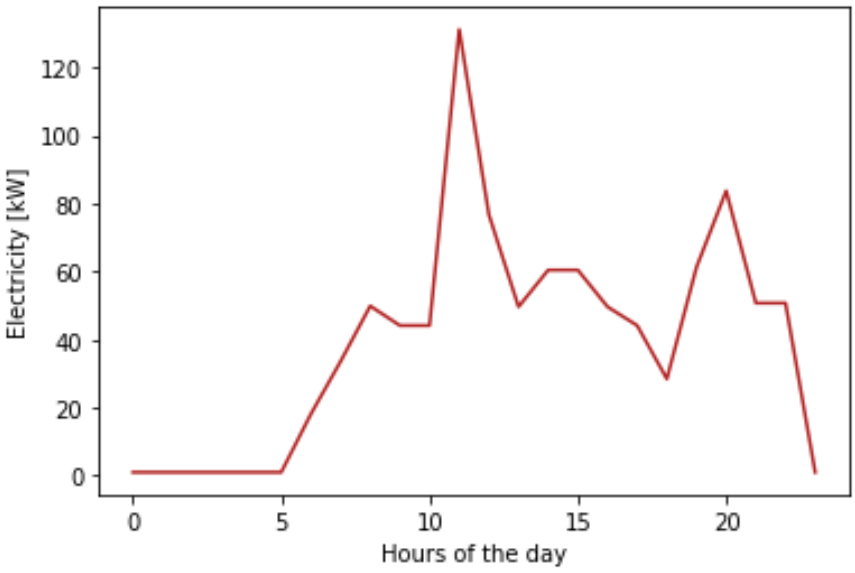

Figure 3.12: Hourly electricity demand from additional loads

3.4.4. Electricity sales and purchase prices

In this study, the electricity purchase price for the hydrogen refuelling station is based on the prepayment tariff for any three-phase calibre applied by the company "Electricité de Guinée (EDG)" to professionals, businesses and industries, specifically for fuel stations in Guinea. The price was set at 1823 GNF/kWh (EDG, n.d.) (GNF: Guinean francs), which is equivalent to 0.2116 $/kWh (US Dollars). Regarding the electricity sales price, the average cost of renewable electricity in the case of ground-mounted PV from Guinea's H2ATLAS project factsheet was taken into account. The cost is 3.9 ct€/kWh (Calow et al., 2010), which is equivalent to 0.0043 $/kWh.

3.4.5. Estimation of hydrogen demand

As stated earlier, the purpose of this study is to assess the practicality of hydrogen refuelling station technology in the country. To date, there are no hydrogen-powered vehicles in Guinea. But, according to the statistics, there is a growing rate of car ownership in Guinea. Almost 40,000 vehicles are registered each year (Emergence Guinée, 2019). Therefore, we can assume that in the future, Guinea may utilize hydrogen-powered vehicles if they become widely available. To define hydrogen demand for fuel cell electric vehicles, it is assumed that vehicles arrive at the refuelling station according to a Poisson process, from 6 a.m. to 10 p.m., giving a constant operating time of 17 hours per day. In addition, the average number of refuelling per hour (or vehicle passages through the refuelling station) is assumed to be 3, and the quantity of hydrogen dispensed per refuelling is assumed to be constant, equal to 5 kg. These presumptions have been used to create the hourly hydrogen demand profile for fuel cell electric vehicles using a Poisson distribution. Poisson distribution is a discrete probability distribution that models the number of times an event occurs in a specified time interval (Sharma et al., 2021). It has two parameters: the rate of occurrence (lambda) and the size of the returned array. With the help of ***numpy.random.poisson()*** method in Python, we can get the random samples from the Poisson distribution and return the random samples by using this method:

$$f(k;\ \lambda) = \frac{\lambda^k e^{-\lambda}}{k!} \qquad (1)$$

This formula returns the probability of observing k events given the parameter λ which corresponds to the expected number of occurrences in that time slot. The syntax in given in equation 2:

$$x = random.poison(lam = \lambda, size = k) \qquad (2)$$

Figure 3.13 shows the generated hourly hydrogen demand profile for fuel cell vehicles.

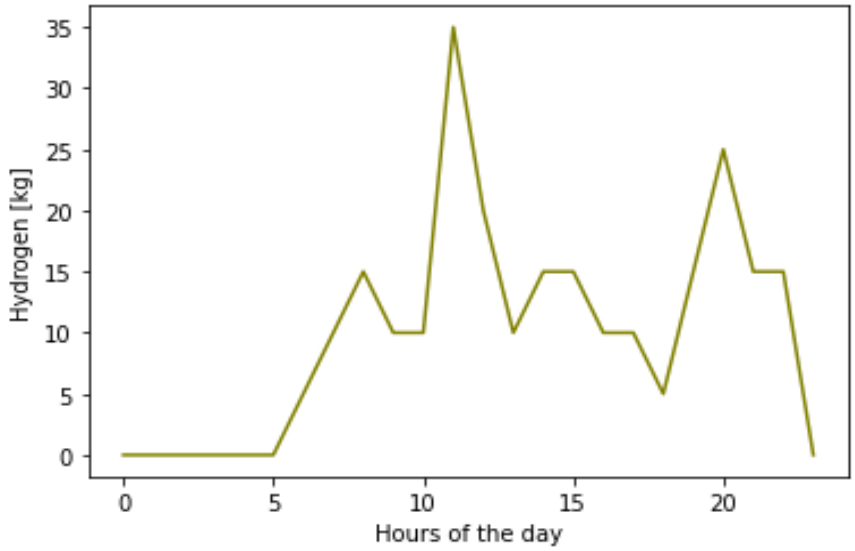

Figure 3.13: Hourly hydrogen demand for FCEVs

3.5. Modelling of the HRS system

Green hydrogen is produced by electrolyzing water in renewable energy-powered refuelling stations that use solar and wind energy. The various key components and interactions within the system are represented by mathematical or computational models.

3.5.1. Modelling of electrolyser

Because of its high energy efficiency, electrolysis is a well-established technique for producing hydrogen, and it can be integrated into energy production systems based on wind and solar energy (Gökçek & Kale, 2018a). To generate electricity for electrolysis, a combination of solar and wind power is used in a hybrid energy system. The process of electrolysis can utilize various sources of water to generate hydrogen. Typically, industrial water such as municipal or groundwater is the preferred source for electrolysis. In this study, it is assumed that a borehole system will be used to carry out electrolysis with groundwater. Proton exchange membrane (PEM) electrolyser was chosen as the hydrogen production system in this study because of its numerous advantages over conventional alkaline water electrolysers. PEM electrolysers can react quickly to power variations and can therefore be easily integrated into renewable energy systems (Gökçek, 2010). Figure 3.14 shows the schematic illustration of the PEM water electrolyser.

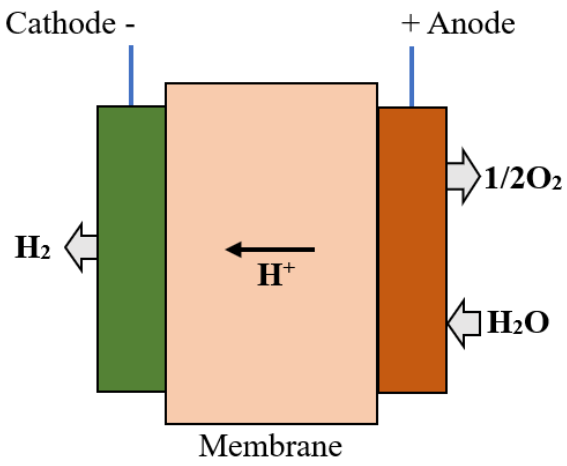

Figure 3.14: Schematic illustration of PEM water electrolyser

Equations 3, 4 and 5 below show the semi-reactions at the anode and cathode and the overall reaction:

- Anode: $H_2O \rightarrow 2H^+ + \frac{1}{2}O_2 + 2e^-$ (3)
- Cathode: $2H^+ + 2e^+ \rightarrow H_2$ (4)
- Overall: $H_2O \rightarrow H_2 + \frac{1}{2}O_2$ (5)

The hydrogen flow rate at the electrolyser outlet is defined using the PEM electrolysers' efficiency formula in equation 6 (Zhang et al., 2012):

$$\eta = \frac{m_{H2,out}LHV}{E} \quad (6)$$

where $m_{H2,\,out}$ is the hydrogen output, LHV is the lower heating value of the hydrogen equal to 33,3 kWh/kg (Fragiacomo & Genovese, 2020), and E is the electrical energy supplied to the PEM electrolyser.

3.5.2. Modelling of water borehole system

As mentioned previously, Guinea has significant water resources, including groundwater (estimated at around 13 billion m³). In this study, it is assumed that groundwater will be used to feed the electrolysis through a borehole system. A water borehole is the best and most common way to obtain groundwater for a variety of purposes. In the water borehole system, the pump is submerged at large depths in narrow holes drilled to extract water from water tables or aquifers located deep underground. The extracted water is pumped into a water storage tank through a supply pipe. The electrolyser will be fed from this tank.

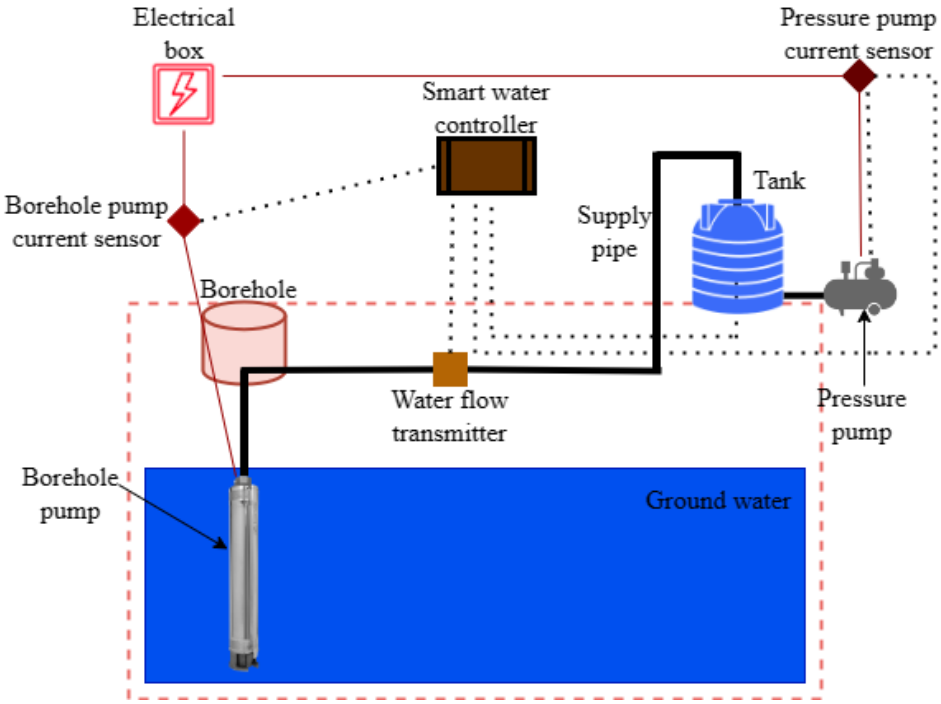

Figure 3.15: Diagram of the borehole system

The output power of the pumping system, given in equation 7, is the hydraulic horsepower transmitted to the fluid by the pump (IEEE Staff & IEEE Staff, 2012).

$$Hydraulic\ Horsepower = Q \times \Delta P \times 1.7 \times 10^{-5} \qquad (7)$$

where Q is the volumetric flow rate through each stage in Barrels per day and ΔP the pressure-rise across the pump in psi.

The efficiency of the entire pump system can be expressed using the following formula:

$$Pump\ System\ Efficiency = \frac{Hydraulic\ Horsepower}{Input\ Power} \qquad (8)$$

where the Input Power refers to the overall amount of electrical power that is provided to the system. This can be calculated using equation 9:

$$Input\ Power = Hydraulic\ Horsepower + S_{Eq,P,losses} + C_{losses} \qquad (9)$$

were, $S_{Eq,\ P,\ losses}$ represents the surface equipment power losses, and C_{losses} the cable losses:

$$C_{losses} = 3I^2R \qquad (10)$$

where I is the operating current per phase of the cable in Amps and R is the total conductor resistance of the cable in Ohms.

Motor input power can be determined from hydraulic horsepower, motor and pump efficiencies as follows:

$$Motor\ Power\ Input = \frac{Hydraulic\ Horsepower}{Eff_{motor} \times Eff_{pump}} \qquad (11)$$

where Eff_{motor} is the efficiency of the motor and Eff_{pump} is the efficiency of the pump. In this study, the motor power input has been estimated in Table 2.

3.5.3. Modelling of renewable energy sources

The PV modules and wind turbines are used as part of the hybrid renewable power generation system in order to supply electricity to the PEM electrolyser and the other electric loads at the hydrogen refuelling station. In a grid-connected system, PV modules and/or wind turbines are linked to an external power grid. This allows the refuelling station to have power even when there is no sun or wind. And any excess electricity generated from renewables is fed back into the grid. The grid-connected system also eliminates the expense of electricity storage devices such as batteries.

Equation 12 provides the hourly power output P_{sj} (in kW) of the PV system given its surface area A_{PV} (in m2) and the total solar radiation of I_{Tj} (in kW/m^2) incident on the PV surface during an average day of the j^{th} month (Bhandari et al., 2015):

$$P_{sj} = I_{Tj} \eta A_{PV} \qquad (12)$$

where the system efficiency η is given by equation 13 (Bhandari et al., 2015):

$$\eta = \eta_m \eta_{pc} P_j \qquad (13)$$

and η_m is the module efficiency which is given by equation 14 (Bhandari et al., 2015):

$$\eta_m = \eta_r [1 - \beta (T_c - T_r)] \qquad (14)$$

η_r is the module reference efficiency, η_{pc} is the power conditioning efficiency, P_f is the power factor, β is the array efficiency, T_r is the reference temperature, and T_c is the monthly average cell temperature.

Equation 15 is the fundamental equation that governs the mechanical power output of a wind turbine (Bhandari et al., 2015):

$$P_{mech} = \frac{1}{2} \rho A C_P V^3 \qquad (15)$$

where ρ is the air density (kg/m^3), A is the swept area of the rotor blades (m^2), V is the wind speed (m/sec) and Cp is the power coefficient of the wind turbine. The theoretical maximum value of the power coefficient Cp is 0.593.

Equation 16 expresses the power output P_{wind} (kW/m^2) of the wind turbine generator (Bhandari et al., 2015):

$$P_{wind} = \begin{cases} P_R \frac{v - v_c}{v_r - v_c}, & for\ (v_c \leq v \leq v_R) \\ P_R\ , & for\ (v_R \leq v \leq v_F) \\ 0, & for\ (v < v_c\ or\ v > v_F) \end{cases} \qquad (16)$$

where P_R is the rated electrical power, v_C is the cut-in wind speed, v_R is the rated wind speed and v_F is the cut-out wind speed.

The actual power available from the wind turbines can be calculated using equation 17 (Bhandari et al., 2015):

$$P = P_{wind} A_{wind} \eta \qquad (17)$$

where A_{wind} is the total swept area and η is the efficiency of the wind turbine generator and associated converters.

Although solar and wind energy sources are environmentally friendly and sustainable, they have an inherent issue of being intermittent and unpredictable. Weather conditions and time of day influence the availability of energy from these sources, making it challenging to maintain a stable and continuous power supply. It is therefore important to use back-up batteries to guarantee a continuous supply of electricity for hydrogen production. The lithium-ion (Li-ion) battery was chosen as the energy storage system in this study because of the many advantages it offers over the lead-acid battery in certain applications. Compared to lead-acid batteries, Li-ion batteries have better discharge characteristics, resulting in a longer lifespan for extracting usable capacity (Kebede et al., 2021).

Battery size depends on factors such as maximum depth of discharge, temperature correction, nominal battery capacity, and battery life (Deshmukh & Deshmukh, 2008). The required battery capacity in ampere-hours is given by equation 18:

$$B_{rc} = \frac{E_{c(Ah)} D_s}{(DOD)_{max} \eta_t} \qquad (18)$$

where $E_{c(Ah)}$ is the load in ampere-hours, D_s is the battery autonomy or storage days, DOD_{max} is the maximum depth of discharge of the battery, and η_t is the temperature correction factor.

The amount of charge in the battery bank at time t can be calculated by equation 19 (Deshmukh & Deshmukh, 2008):

$$E_B(t) = E_B(t-1)(1-\sigma) + \left(\frac{E_{GA}(t) - E_L(t)}{\eta_{inv}}\right)\eta_{bat} \qquad (19)$$

where $E_B(t)$ and $E_B(t\text{-}1)$ are the amounts of charge in the battery bank at time t and $t\text{-}1$, $\boldsymbol{\sigma}$ is the hourly self-discharge rate, $E_{GA}(t)$ is the total energy generated by the renewable energy source after the loss of energy in the controller, $E_L(t)$ is the load demand at time t, η_{inv} and η_{bat} are the inverter efficiencies and the charging efficiency of the battery bank.

The state of charge (SOC) of the battery at a time (t) can be calculated using equation 20 (Bhandari et al., 2015):

$$SOC(t) = SOC(t-1) \times \left(1 - \frac{\sigma \times \Delta t}{24}\right) + \frac{I_{bat}(t-1) \times \Delta t \times \eta_{bat}}{C'_{bat}} \qquad (20)$$

where C'_{bat} is the nominal capacity of the battery (Ah) and η_{bat} is the charging and discharging efficiency of the battery.

3.5.4. Modelling of DC-AC converter

The DC-AC converter is used to convert direct current (DC) coming from PV modules and batteries to alternating current (AC) through a process known as inversion (HOMERHelpManual, 2016). The electricity output of the DC-AC converter is expressed using its efficiency formula as in equation 21:

$$\eta_{conv} = \frac{P_{AC}}{P_{DC}} \qquad (21)$$

where P_{AC} is the AC output electrical power and P_{DC} is the DC input electrical power.

3.5.5. Modelling of hydrogen compressor

Hydrogen refuelling stations are designed to fill the storage tank of fuel cell electric vehicles at 700 bars for light-duty vehicles or 700 bars, for all other vehicles while the output pressure for commercial PEM electrolysers is from 14 to 50 bars (Sun & Harrison, 2021) and (Gökçek & Kale, 2018b). Therefore, compressors that are capable of compressing hydrogen gas from the outlet pressures of the electrolysers to these higher pressures (minimum 300 bars) are required.

The compressor's energy consumption can be calculated according to equation 22 (Gökçek & Kale, 2018a):

$$W_{comp} = C_p \frac{T_1}{\eta_c}\left[\left(\frac{P_2}{P_1}\right)^{\frac{r-1}{r}} - 1\right] m_{H_2,c} \qquad (22)$$

where C_p is the specific heat of hydrogen at constant pressure (14.304 kJ/kg ^oK), T_1 is the inlet gas temperature of the hydrogen compressor (293 ^oK), η_c is the compressor efficiency, P_1 and P_2 represent the inlet and output gas pressures of the hydrogen compressor, respectively, r is the isentropic exponent of hydrogen (r = 1.4), and $m_{H2,\,c}$ is the gas flow rate through the hydrogen compressor in kg/s.

3.5.6. Modelling of hydrogen storage tank

Hydrogen storage tanks are required to store the hydrogen produced since this hydrogen can be used at any time to refuel fuel cell electric vehicles. Hydrogen can be stored in three different ways: i) as a gas under high pressures, ii) in liquid form under cryogenic temperatures and, iii) on the surface of or within solid and liquid materials (TWI, 2023). For this study, it is assumed that the produced hydrogen will be stored in gaseous form at high-pressure thanks. Compressed hydrogen storage involves storing hydrogen in a gaseous form under high pressures (usually between 350 and 700 bar) in a robust pressure tank (EERE, 2023). Modelling compressed hydrogen storage is crucial for the development of efficient and safe hydrogen storage systems. Within the optimization software, the size of the storage tank is determined based on the amount of hydrogen required to meet the refuelling needs of the station.

The following forms can be used to write the mass and energy balance equations for hydrogen gas stored in a tank (Xiao et al., 2016, 2019):

$$\frac{dm}{dt} = \dot{m_{in}} - \dot{m_{out}} \qquad (23)$$

$$\frac{d}{dt}(mu) = \dot{m_{in}} h_{in} - \dot{m_{out}} h_{out} + \dot{Q} \qquad (24)$$

where m_{in} and m_{out} are respectively the hydrogen mass flow rates in which the hydrogen flows into the inlet and outlet of the tank, h_{in} and h_{out} are respectively the specific enthalpy of inflow and outflow hydrogen, and Q is the heat inflow rate.

3.5.7. Modelling of hydrogen dispensing system

Hydrogen dispensers transfer hydrogen from high-pressure tanks to the onboard high-pressure hydrogen tanks of hydrogen fuel cell electric vehicles using 350- or 700-bar nozzles (Alazemi & Andrews, 2015). During the hydrogen filling process, the Joule-Thomson coefficient is negative, resulting in an increase in gas temperature during an isenthalpic filling expansion. As a result, the temperature of the hydrogen also increases significantly (Farzaneh-Gord et al., 2012). Pre-cooling is necessary to prevent temperature increases in fuel cell electric vehicles' tanks during expansion to maintain safety (use of pre-cooling unit PCU). The dispenser type considered in this study is B70. It complies with the SAE TIR J2601 worldwide hydrogen fuelling protocol as it can refuel at 700 bars with hydrogen pre-cooled at - 20 ºC (Nistor et al., 2016). The proposed hydrogen dispenser system includes two main components: the refrigeration system, which cools the hydrogen before delivery, and the dispenser nozzle, which controls the flow of gas into the hydrogen vehicle.

The cooling power requirement of the dispenser while fuelling a vehicle can be determined using equation 25 (Minutillo et al., 2021):

$$P_{cool} = \dot{m_{H_2,D}}\left(h_{storage} - h_{dispenser}\right) \qquad (25)$$

where $m_{H2,\,D}$ is the hydrogen flow at the dispenser, and h is the enthalpy at the storage and dispenser outlet. According to (Minutillo et al., 2021) calculations, the cooling power required in this study to lower the hydrogen temperature in the dispenser is 16.3 kW.

The calculation for the electric power supplied to the refrigeration system is as follows (Minutillo et al., 2021):

$$P_{refrigerator} = \frac{P_{cool}}{COP} \qquad (26)$$

where *COP* stands for coefficient of performance, equal to 1.0.

3.5.8. Modelling, problem formulation and optimisation using COMANDO

All the optimisation processes were carried out using the COMANDO software on a laptop with the default settings. The laptop specifications are shown in Figure 3.16. COMANDO is an open-source Python package for component-oriented modelling and optimization for nonlinear design and operation of integrated energy systems, which allows to assemble system models from component models including nonlinear, dynamic and discrete characteristics (Langiu et al., 2021).

Device name	LENOVO
Processor	Intel(R) Core(TM) i7-10510U CPU @ 1.80GHz 2.30 GHz
Installed RAM	16.0 GB (15.8 GB usable)
Device ID	D931DBE0-174A-4A02-8B0A-B670D81F666B
Product ID	00330-80139-51627-AA949
System type	64-bit operating system, x64-based processor
Pen and touch	No pen or touch input is available for this display

Figure 3.16: Specifications of the laptop used for optimization

The usage of COMANDO can be split into three phases: modelling, problem formulation, and problem solution (Langiu et al., 2021):

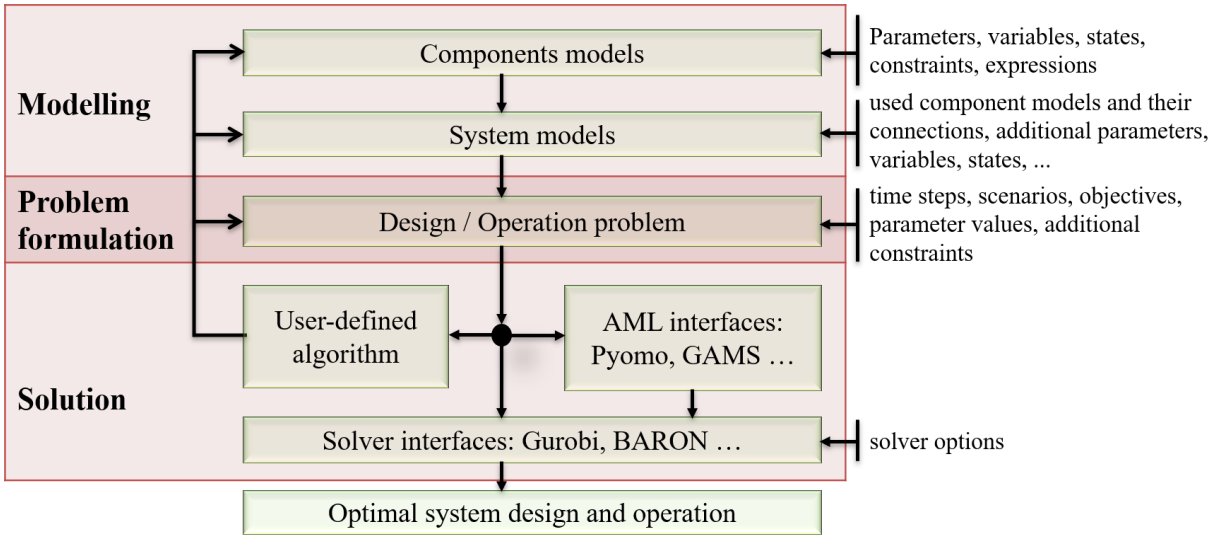

Figure 3.17: COMANDO operating phases

(1) **Modelling process:** To begin, we describe component models, which represent elementary energy system components. A component model consists of mathematical expressions in symbolic form, representing parameters or design or operational variables, placeholders for values to be determined during optimization. Different component models can be combined into a system model by specifying the connections between them.

(2) **Problem formulation:** By using a completed system model, various optimization problems can be generated considering the design and/or operation of the system. In this study, the design variables considered are the sizes of the main components of the refuelling station (PV modules, wind turbines, converters, electrolysers, batteries, compressors and hydrogen storage tanks). The operational variables include the output of electricity generated by PV modules and wind turbines; input and output of electricity, along with the

state of charge for batteries; input of electricity and output of hydrogen for electrolysers; input and output of electricity for converters; input of electricity, input and output of hydrogen for compressors; input and output of hydrogen for hydrogen storage tanks; and purchase and sale of electricity for the power grid.

The optimization problem consists of two primary objective functions: the design objective (*Desg_Obj*) and the operational objective (*Oper_Obj*):

$$Desg\_Obj = \sum_i Fix\_Costs + \sum_i Inv\_Costs + \sum_i Rep\_Costs \quad (27)$$

$$Oper\_Obj = \sum_i Var\_Costs \quad (28)$$

where *Fix_Costs* represents the fixed costs of component *i*; *Inv_Costs*, the annualized capital expenditures of component *i*; *Rep_Costs*, the annualized replacement costs of component *i*; and *Var_Costs* refers to the variable costs, including the cost of electricity purchased from the grid and the cost of electricity sold to the grid.

To make green hydrogen a more competitive alternative to fossil fuels, the goal of the optimization problem is to minimize variable costs through efficient operations and the use of cost-effective renewable energy sources. The objective function is formulated to minimize the total cost associated with various components and operations of the station while meeting performance requirements.

$$OF = Minimize(Desg\_Obj, Oper\_Obj) \quad (29)$$

(3) **Problem solution:** After the problem is formulated, it can directly be passed to an algebraic modelling language using AML interfaces, such as Pyomo and GAMS, or directly to a suitable solver, such as the Gurobi and BARON. The problem can also be addressed using a user-defined algorithm, ranging from simple preprocessing routines based on the system model and available data to advanced methods like decomposition techniques in stochastic programming.

3.6. Techno-economic analysis

A techno-economic analysis is carried out on the basis of the net present cost (NPC) and the levelized cost of hydrogen (LCOH), in order to comprehensively assess the feasibility, profitability and potential environmental benefits of setting up and operating green hydrogen refuelling stations powered by renewable energies for hydrogen-powered vehicles. The NPC and LCOH are affected by the size of the system and the per-unit cost of the different components (Barhoumi et al., 2022).

3.6.1. The net present cost (NPC)

The NPC of the system represents the difference between the present value of all the costs of installing and operating the system and the present value of all the revenues it generates over its lifetime (Gökçek & Kale, 2018a). It is calculated as follows:

$$NPC = \frac{C_{ann,tot}}{CRF} \qquad (30)$$

where $C_{ann,\ tot}$ represents the total annual cost of the system, and *CRF* represents the capital recovery factor. The $C_{ann,\ tot}$ and the *CRF* were calculated using equations 28 and 29, respectively:

$$C_{ann,tot} = C_{ann,inv} + C_{ann,rep} + C_{O\&M} - Rev_{el} \qquad (31)$$

$$CRF = \frac{i(1+i)^n}{(1+i)^n - 1} \qquad (32)$$

- $C_{ann,\ rep}$ is the annualized replacement costs;

$$C_{ann,rep} = CRF \times \frac{C_{rep}}{(1+i)^t} \qquad (33)$$

  where C_{rep} and *t* are the replacement cost and related year, respectively.
- $C_{O\&M}$ is the operating and maintenance costs, calculated on a yearly basis;
- Re_{vel} represents the annual revenue obtained by selling electricity excess from renewables;
- *i* represents the real discount rate, equal to 11.5 % (Trading Economics, 2023);
- *n* represents the project lifetime (assumed to be 25 years);
- $C_{ann,\ inv}$ is the annualized investment cost, calculated using equation 31:

$$C_{ann,inv} = C_{inv} \times CRF \qquad (34)$$

  where C_{inv} represents the total plant capital investment costs.

3.6.2. The levelized cost of hydrogen (LCOH)

LCOH is defined as the ratio between the total annualised costs of the system and the annual amount of hydrogen produced (Caponi et al., 2022). By calculating the LCOH, we can assess the economic effectiveness of different configurations of the HRS and choose the one with the lowest cost of hydrogen production (Minutillo et al., 2021). It is calculated using the general equation 32:

$$LCOH = \frac{C_{ann,tot}}{\sum m_{ann,H_2,prod}} \qquad (35)$$

were $m_{ann,\ H2,\ prod}$ represents the annual amount of hydrogen produced.

3.7. Limitations

In this section, different factors that have impacted the scope of this study will be we will be discussed. The main limitation of this study is the time factor. The study was carried out at the Institute of Energy and Climate Research (IEK-10) institute in the research centre Forschungszentrum Jülich GmbH during a 4-month stay in Germany. Far from the study area and within a limited time frame, the time factor affected different aspects of the research process and could influence the results of the study:

- **Data collection:** The limited time available resulted in a limited amount of collected data. As a result, a life-cycle assessment, such as the global warming impact of the systems that represent CO_2 emissions, could not be carried out due to the lack of data.
- **Data analysis:** The time constraints restricted the depth of data analysis. Certain steps such as the sensitivity analysis, which allows to determine the impact of various parameters on the obtained results (Rabiee et al., 2021), have not been performed in this study due to time constraints.

This study subsequently relied solely on the collected data and the most relevant analysis.

4. Chapter 3: Results and discussion

The purpose of this chapter is twofold. Firstly, the main findings of the data collection, processing and analysis are concisely and objectively described in the results section. Next, the discussion section explains the significance, importance and relevance of the results, in relation to what is already known in the subject area and with the expected results.

4.1. Results

4.1.1. Optimization results

4.1.1.1. Components sizing

The optimum sizes of the main components for each configuration of the HRS are reported in Table 4.1.

Table 4.1: Sizing of the main HRS system components

	Hybrid PV-wind & battery system	Grid-connected PV system	Stand-alone PV & battery system
PV modules [kW]	8168	7235	8500
Wind turbines [kW]	405.8	-	-
Converter [kW]	205.2	142.7	225.7
Electrolyser [kW]	1162	1244	1189
Lit. ion battery [kWh]	278.1	-	324.5
Compressor [kW]	84.07	90	86.02
H2 Storage tank [kg]	84.67	89.56	90.13

4.1.1.2. Production and use of electricity

The optimization results for electricity generation and demand within the hybrid PV-wind and battery system, the grid-connected PV system and the stand-alone PV and battery system are depicted in Figures 4.1, 4.2 and 4.3, respectively. The positive values represent the electricity supply which includes generation from the PV park, wind farm (in a hybrid system), the power grid (in a grid-connected system), and battery discharging. Electricity demand is shown as negative values, which includes energy needed for electrolysers, compressors, electrical loads at the HRS, and battery charging. In the grid-connected PV system, the total amount of electricity purchased from the grid annually is 104,652 kWh, while the amount of electricity sold to the grid annually is 40,251 kWh.

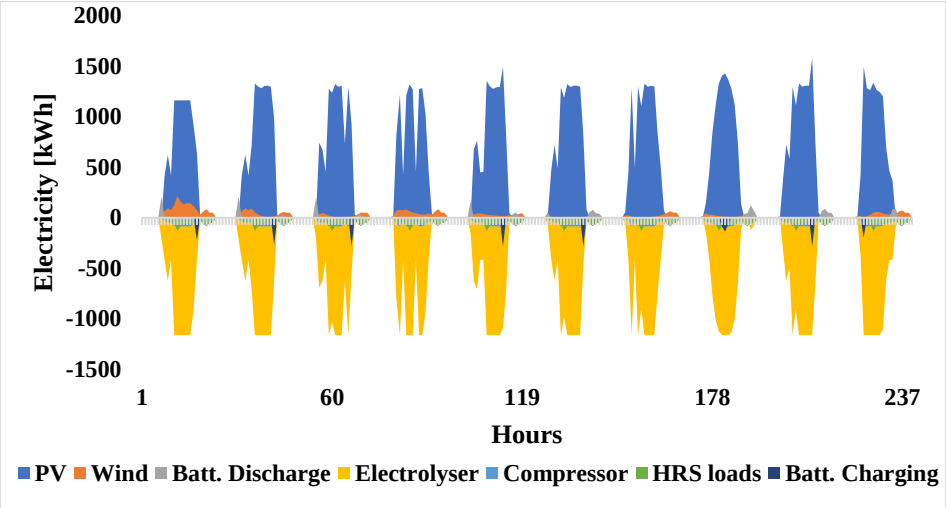

Figure 4.1: Electricity generation and demand within the hybrid PV-wind and battery system

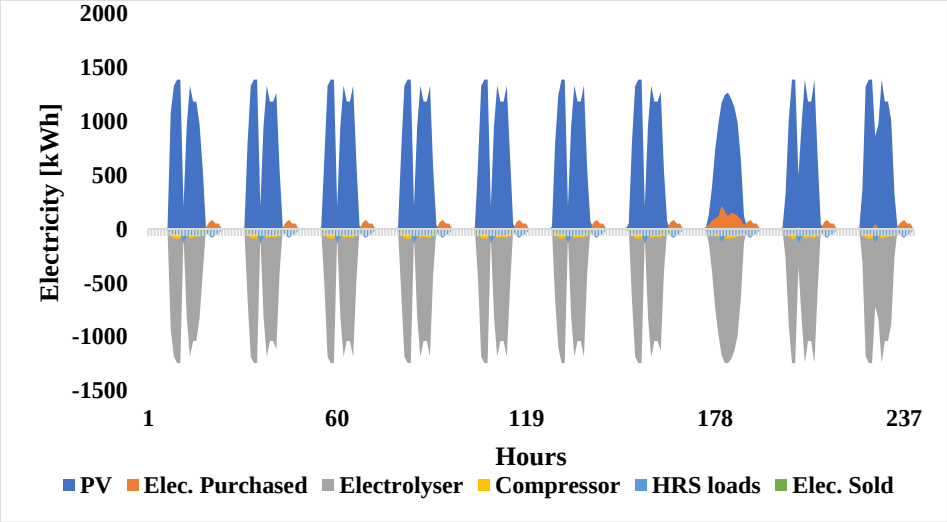

Figure 4.2: Electricity generation and demand within the grid-connected PV system

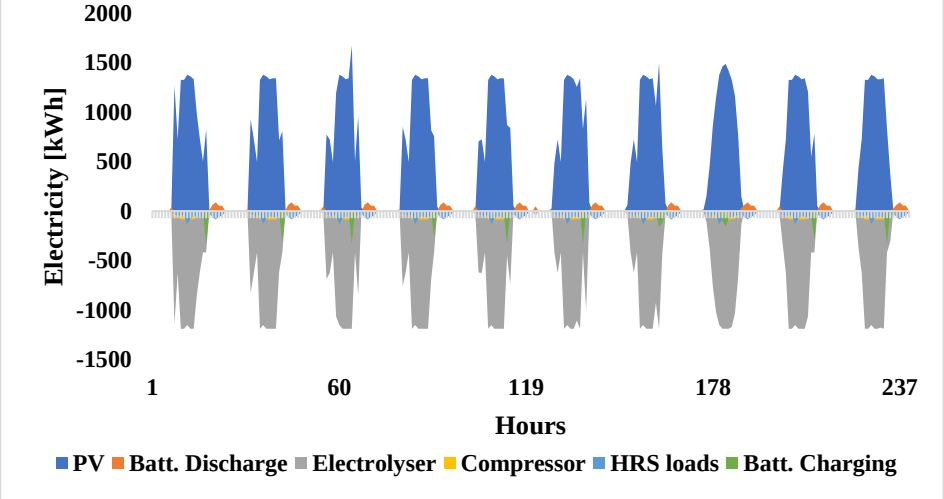

Figure 4.3: Electricity generation and demand within the stand-alone PV-battery system

4.1.1.3. Production and use of hydrogen

The optimization results show that in each configuration, the total amount of hydrogen produced per year by the hydrogen refuelling station is 87,600 kg. The profiles of hydrogen production, storage, de-storage, and refuelling for the hybrid PV-wind and battery system, the grid-connected PV system, and the stand-alone PV and battery system are depicted in Figures 4.4, 4.5, and 4.6, respectively. In this case, positive values represent the production and de-storage of hydrogen (electrolyser and hydrogen tank outlets), while negative values represent the demand and storage of hydrogen (demand for FCEVs and hydrogen tank inlet).

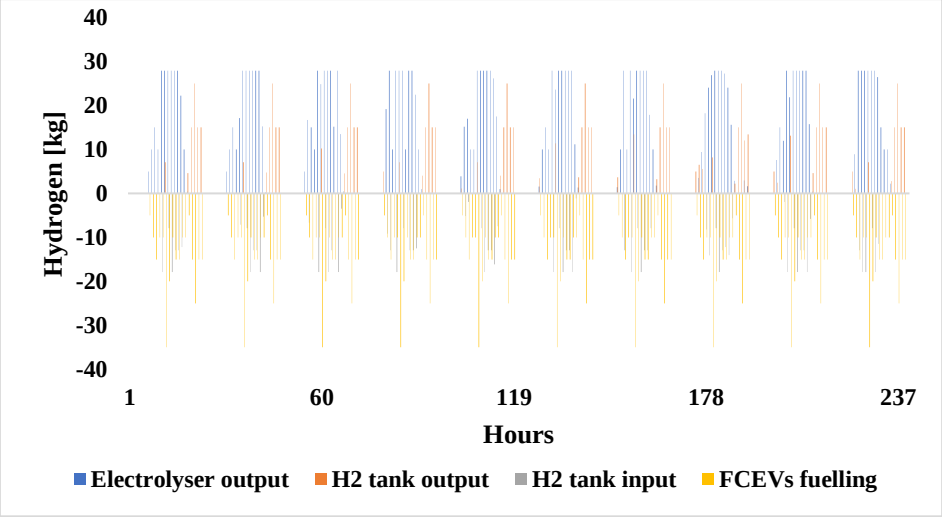

Figure 4.4: Hydrogen production, storage, de-storage, and refuelling for hybrid PV-wind and battery system

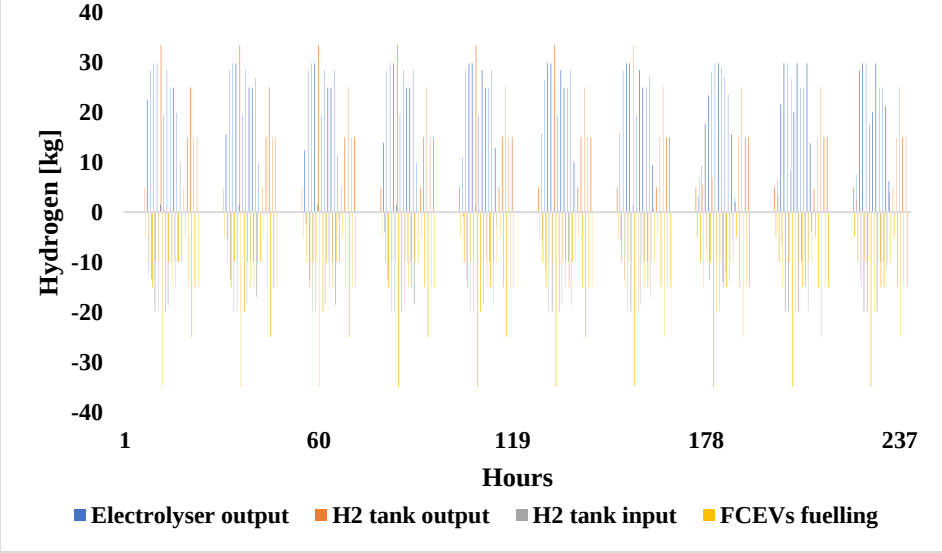

Figure 4.5: Hydrogen production, storage, de-storage, and refuelling for grid-connected PV system

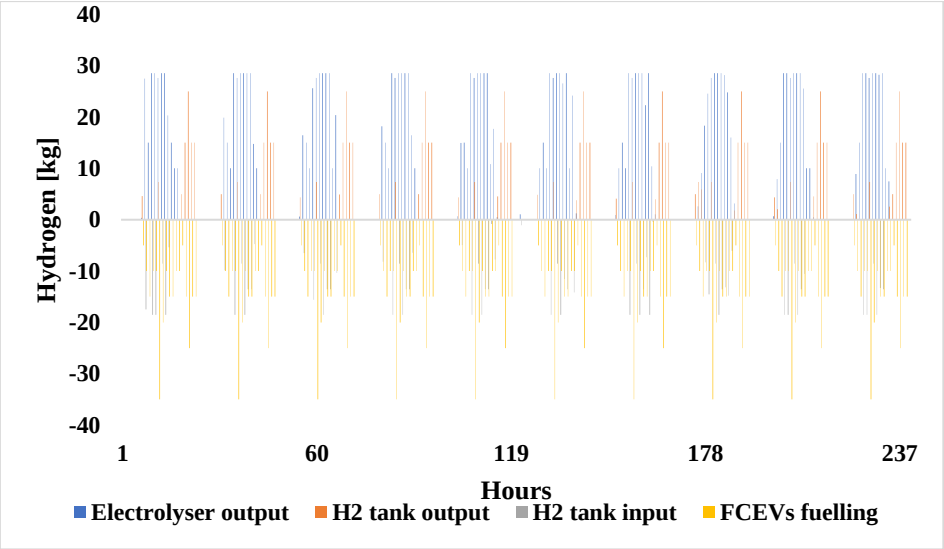

Figure 4.6: Hydrogen production, storage, de-storage, and refuelling for stand-alone PV-battery system

4.1.2. Techno-economic analysis results

The total initial investment costs for the main components of the hydrogen refuelling station system for each configuration are shown in Table 4.2.

Table 4.2: Investment costs of the main HRS system components

	Hybrid PV-wind & battery system	Grid-connected PV system	Stand-alone PV & battery system
PV modules [k$]	6942.8	6149.75	7225
Wind turbines [k$]	405.8	-	-
Converter [k$]	114.16	79.39	125.56
Electrolyser [k$]	976.08	1044.96	998.76
Lit. ion batterie [k$]	302.3	-	352.73
Compressor [k$]	210.18	225	215.05
H2 Storage tank [k$]	122.6	129.68	130.51
Dispenser with PCU [k$]	340	340	340
Water borehole [k$]	19.29	19.29	19.29

The total initial investment costs of the installation, which correspond to all the expenditure required to set up the hydrogen refuelling station for each configuration, and their annualised values, calculated taking into account the lifetime of the installation and the real discount rate, are presented in Table 4.3.

Table 4.3: Total plant capital investment costs and annualized values

	Hybrid PV-wind & battery system	Grid-connected PV system	Stand-alone PV & battery system
Total initial inv. Costs [k$]	9433.2	7988.07	9406.9
Total annual. inv. Costs [k$/year]	1161.21	983.32	1157.97

The total annual cost refers not only to the total initial investment due to plant construction but also all the management costs (operating and maintaining costs) over the entire lifetime (Minutillo et al., 2021). Table 4.4 presents the total annual costs of the HRS system for each configuration.

Table 4.4: Total annual costs of the HRS system

	Hybrid PV-wind & battery system	Grid-connected PV system	Stand-alone PV & battery system
Total annualized costs [k$]	6865	5889	6980

The optimization results for net present cost (NPC) and the levelized cost of hydrogen (LCOH), which will enable the comparison of the three configurations analysed and the selection of the optimal solution (Barhoumi, Okonkwo, Ben Belgacem, et al., 2022), are grouped in Table 4.5.

Table 4.5: NPC and LCOH for each configuration

	Hybrid PV-wind & battery system	Grid-connected PV system	Stand-alone PV & battery system
LCOH [$/kg]	3.13	2.69	3.19
NPC [k$]	55766	47836	56702

4.2. Discussion

This study focuses on designing a hydrogen refuelling station that can meet the hydrogen demand of fuel cell electric cars. Three different renewable power generation systems, including a hybrid PV-wind and battery system, a grid-connected PV system, and a stand-alone PV and battery system, were explored to determine the best option for producing green hydrogen using solar and wind energy.

Designing a hydrogen refuelling station requires careful consideration of component sizing, which is a crucial aspect to ensure optimal performance. The optimization results for the sizing of the components are presented in Table 4.1. These results present the capacities of

electrolysers, storage tanks, compressors, and other relevant components to ensure efficient hydrogen production and storage needed to meet the demand for hydrogen vehicles. It is noted that the PV modules are most solicited compared to wind turbines in the hybrid PV and wind system. This is primarily due to the high investment costs associated with wind energy and the availability of solar potential compared to wind. The Atlantic Ocean coastal regions of Guinea Conakry experience the highest wind velocity, whereas the northeastern regions receive the most sunshine. In the area under study, which is in the country's northern region, solar energy production is more lucrative than wind power. Furthermore, the largest size of photovoltaic modules is observed in the stand-alone photovoltaic system with batteries. This is mainly due to the absence of a grid connection and the high cost of batteries. As the solar energy potential is high, a larger size of PV modules is required to meet the electricity demand of the installation. The battery is only needed to store excess electricity and supply it when the sun is not available. The lowest size of PV modules is observed in the grid-connected system.

Understanding the electricity production and demand patterns is crucial for the effective evaluation of renewable energy sources. The optimization results for electricity generation and demand within each HRS system depicted in Figures 4.1, 4.2 and 4.3 offer a thorough understanding of the amount of renewable energy capacity needed to generate the necessary hydrogen and fulfil the operational requirements of the refuelling station. It is noted that in each configuration, the high amount of electricity produced by the PV modules is utilized almost entirely for powering the electrolyser, while other energy sources like wind and grid are utilized for the requirements of other components.

The hydrogen production and utilization process is a central aspect of this study. The purpose of the HRS system is to generate hydrogen that can be used to refuel fuel cell vehicles. The hydrogen produced by the electrolysers is either utilized immediately or kept in designated storage tanks for future use. As depicted in Figures 4.4, 4.5 and 4.6, the storage tank in each HRS system configuration stores the hydrogen produced by the electrolyser's outlet. At any time, the amount of hydrogen stored is the difference between the produced amount and the amount needed to refuel the FCEVs. This stored hydrogen is utilized to meet the demand for FCEVs when the electrolyser is not functioning.

A crucial factor in determining whether it is feasible to build green hydrogen refuelling stations is the initial investment costs. Tables 4.2 and 4.3 provide a summary of the main component costs, total initial investment costs, and total annualized investment costs for each HRS system configuration. These results provide a comprehensive view of the financial

implications of setting up the hydrogen refuelling station. The grid-connected PV system has the lowest initial investment cost equal to 7,988,070 $. Whereas the initial investment costs of the hybrid PV-wind and battery system and the stand-alone PV and battery system are 9,433,200 $ and 9,406,900 $, respectively. Table 4.4 presents the overall yearly expenses for the HRS system, encompassing operational and maintenance costs, along with possible potential earnings from the sale of renewable electricity. The results provide a clear understanding of the ongoing financial responsibility needed to maintain the station's operation. The grid-connected PV system has the lowest total annual cost, amounting to 5,889,000 $. On the other hand, the total annual costs of the hybrid PV-wind and battery system and the stand-alone PV and battery system are 6,865,000 $ and 6,980,000 $, respectively.

The Net Present Cost (NPC), which factors in interest rates and discounts future costs and benefits, helped us compare the lifetime costs of various HRS systems. The Levelized Cost of Hydrogen (LCOH), on the other hand, is an important measurement for comparing the cost of producing hydrogen from renewable sources with that of other conventional fuel sources. The optimization results for NPC and LCOH are summarized in Table 4.5. The NPC of the grid-connected PV system is 47,836,000 $, which is the lowest. In contrast, the NPCs of the hybrid PV-wind system and the stand-alone PV and battery system are 55,766,000 $ and 56,702,000 $, respectively. The high operating and initial investment costs of the stand-alone photovoltaic and battery system are mainly responsible for the high NPC of this system. The LCOH of the grid-connected PV system is 2.69 $/kg. The LHC for the hybrid PV-wind system and the stand-alone PV and battery system are 3.13 $/kg and 3.19 $/kg, respectively. Overall, it can be concluded that the grid-connected PV system offers the most cost-effective and efficient option with the lowest LCOH. The technical and economic specifications of the optimal grid-connected PV hydrogen refuelling station are summarized in Table 4.6.

Table 4.6: Technical and economic specifications of the grid-connected PV-HRS

Components	Rated capacity	Capital cost [k$]	Replacement cost [k$]	O&M cost [k$]	Total cost [k$]
PV modules	7235 kW	6149.75	0	4160.13	10309.88
Converter	142.7 kW	79.39	1.91	3.92	85.22
Electrolyser	1244 kW	1044.96	25.13	653.1	1723.19
Compressor	90 kW	225	0	112.5	337.5
Storage tank	89.56 kg	129.68	0	6.72	136.4
Dispenser with PCU	16.3 kW	340	4.74	26	370.74
Water borehole	5.5 kW	19.29	0	19.28	38.57

The total cost of installing and maintaining PV modules is $10,309,880. The required power of the electrolyser is 1,244 kW, which has a cost of 1,723,190 $. The hydrogen tank, compressor and converter cost a total of 136,400 $, 337,500 $ and 85,220 $ respectively.

The technical and economic specifications of the two other HRS configurations: the hybrid PV-wind and battery system and the stand-alone PV and battery system are summarized in Table 4.7 and 4.8 respectively.

Table 4.7: Technical and economic specifications of the hybrid PV-wind and battery HRS

Components	Rated capacity	Capital cost [k$]	Replacement cost [k$]	O&M cost [k$]	Total cost [k$]
PV modules	8168 kW	6942.8	0	4696.6	11639.4
Wind turbines	405.8 kW	405.8	0	121.74	527.54
Converter	205.2 kW	114.16	2.75	5.64	122.55
Electrolyser	1162 kW	976.08	23.48	610.05	1609.61
Lit. ion Batterie	278.1 kW	302.3	10.67	188.94	501.9
Compressor	84.07 kW	210.18	0	105.09	315.27
H2 Storage tank	84.67 kg	122.6	0	6.35	128.95
Dispenser & PCU	16.3 kW	340	4.74	26	370.74
Water borehole	5.5 kW	19.29	0	19.28	38.57

Table 4.8:Technical and economic specifications of the stand-alone PV and battery HRS

Components	Rated capacity	Capital cost [k$]	Replacement cost [k$]	O&M cost [k$]	Total cost [k$]
PV modules	8500 kW	7225	0	4887.5	12112.5
Converter	225.7 kW	125.56	3.02	6.21	134.79
Electrolyser	1189 kW	998.76	24.02	624.23	1647.01
Lit. ion Batterie	324.5 kW	352.73	7.22	220.46	580.41
Compressor	86.02 kW	215.05	0	107.53	322.58
H2 Storage tank	90.13 kg	130.51	0	6.76	137.27
Dispenser & PCU	16.3 kW	340	4.74	26	370.74
Water borehole	5.5 kW	19.29	0	19.28	38.57

In the hybrid PV-wind and battery HRS, the cost of installing and maintaining PV modules and wind turbines is 11,639,400 $ and 527,540 $, respectively. The required power of the electrolyser is 1,162 kW, which costs 1,609,610 $. The hydrogen tank, compressor and converter cost a total of 128,950 $, 315,270 $ and 122,550 $, respectively. On the other hand, in the stand-alone PV and battery HRS, the cost of installing and maintaining PV modules is 12,112,500 $. The electrolyser requires 1,189 kW of power and costs 1,647,010 $, while the hydrogen tank, compressor, and converter cost 137,270$, 322,580$ and 134,790$, respectively.

5. Conclusion and recommendations

5.1. Conclusion

Green hydrogen is a promising alternative to traditional transportation methods to achieve net zero targets. It can decrease CO_2 emissions, and fossil fuel dependence, and boost the energy sector's economy, particularly in developing countries. However, the high cost of production is limiting hydrogen-based renewable initiatives. Consequently, optimizing the operation of green hydrogen refuelling stations is critical in balancing renewable energy production, and hydrogen storage capacity, and reducing production costs. This master study aimed to determine the best solution for producing green hydrogen for refuelling stations using renewable energy sources. The sub-prefecture of Baté-Nafadji in Guinea Conakry has been used as a case study to analyse three different technical solutions that can be used to produce green hydrogen using solar and wind energy. Starting with a thorough examination of the scientific literature, the major contribution of the transport sector to climate change has been first discussed. Next, the importance of green hydrogen as a promising answer to the challenges of energy transition, mitigating climate change, and promoting sustainable development has been emphasized.

The solar and wind data used for the simulations were collected over a year using the Renewables.ninja web tool. Technical and economic information on the components was obtained from open sources and literature. Other data, such as the hydrogen demand for fuel cell electric vehicles, were estimated using assumptions. The three-hybrid renewable power generation systems proposed for feasibility and optimization of hydrogen production are the hybrid PV wind and battery system, the grid-connected PV system, and the stand-alone PV and battery system. The analysis was carried out using the COMANDO open-source framework for energy systems optimization.

The economic analysis shows that the grid-connected PV system has the lowest NPC and LCOH, while stand-alone PV and battery system have the highest. However, the LCOH of the hybrid PV-wind system with battery is higher than a grid-connected PV system but lower than a stand-alone PV and battery system. The three configurations of hydrogen production are economically viable for the Baté-Nafadji sub-prefecture compared to renewable-powered hydrogen refuelling stations mentioned in the literature. In contrast to traditional power generation systems, three alternative options have been proposed to reduce gas emissions. Stand-alone PV and battery systems, as well as hybrid PV-wind and battery systems, produce

no gas but are more expensive compared to the grid-connected PV system. The optimized solution shows a grid-connected PV hydrogen refuelling station with a capacity of 7.24 MW can generate 87,600 kg of green hydrogen annually, with an LCOH of 2.69 $/kg and a total NPC of 47,836,000 $. Given the results above, a grid-connected PV hydrogen refuelling station is a suitable technology for producing green hydrogen in the Baté-Nafadji sub-prefecture, Guinea, using renewable energy sources.

This study presents a comprehensive optimization model for renewable energy sources, hydrogen demand, storage technologies, and station components, making it one of the first studies to explore this technology in the country and on the entire continent of Africa. Overall, this study found sustainable energy solutions for efficient resource utilization, technological advancement, policy formulation, economic viability, and promoting hydrogen vehicle adoption. In real life, this study may assist policymakers and stakeholders in making informed decisions regarding the effective allocation of resources, setting targets, and providing incentives for green hydrogen production in Guinea.

5.2. Recommendations

Research into the optimal sizing of green hydrogen refuelling stations powered by renewable energy for hydrogen vehicles is an important area that can contribute to the development of sustainable transport and energy systems. Given the insights gained from this research, some recommendations could be formulated for further research:

- **Sensitivity analysis:** Conduct sensitivity analysis to determine how changes in input parameters impact model outcomes, increasing the reliability and robustness of decision-making.
- **Environmental impact:** Perform life cycle assessment (LCA) on hydrogen refuelling stations powered by renewable energy sources to evaluate their environmental impact. This evaluation should take into account factors such as carbon footprint, water usage, and other relevant factors to determine overall sustainability.
- **Integrating an AC power:** Address the same topic, by integrating an AC power flow in the optimization framework COMMANDO to be able to accurately represent the physical behaviour of energy systems.
- **Hydrogen revenue:** Integrate hydrogen revenue to find a balance between maximizing revenue from hydrogen sales, minimizing environmental impact, and ensuring the station's economic viability.

Bibliography references

AdeleT. (2018). *How much does a borehole cost? - Springhill Water - Boreholes, Spring Water & Pumps*. https://privatewatersupplies.org.uk/how-much-does-a-borehole-cost/

AEO. (2023). *African Economic Outlook 2023: Mobilizing Private Sector Financing for Climate and Green Growth in Africa.* Page 212.

Ajanovic, A., & Haas, R. (2021). *Prospects and impediments for hydrogen and fuel cell vehicles in the transport sector. International Journal of Hydrogen Energy*, *46*(16), 10049–10058. https://doi.org/10.1016/j.ijhydene.2020.03.122

Alazemi, J., & Andrews, J. (2015). *Automotive hydrogen fuelling stations: An international review. Renewable and Sustainable Energy Reviews*, *48*, 483–499. https://doi.org/10.1016/j.rser.2015.03.085

Alsayegh, O. A. (2021). *Barriers facing the transition toward sustainable energy system in Kuwait. Energy Strategy Reviews*, *38*, 100779. https://doi.org/10.1016/j.esr.2021.100779

Apostolou, D., & Xydis, G. (2019). *A literature review on hydrogen refuelling stations and infrastructure. Current status and future prospects. Renewable and Sustainable Energy Reviews*, *113*, 109292. https://doi.org/10.1016/j.rser.2019.109292

ARUP. (n.d.). *The Future of Energy - Green hydrogen transport - Arup - Arup. Web page viewed on 12 July 2023*. Retrieved July 12, 2023, from https://www.arup.com/perspectives/publications/research/section/the-future-of-energy-green-hydrogen-transport

Ayodele, T. R., Mosetlhe, T. C., Yusuff, A. A., & Ntombela, M. (2021). *Optimal design of wind-powered hydrogen refuelling station for some selected cities of South Africa. International Journal of Hydrogen Energy*, *46*(49), 24919–24930. https://doi.org/10.1016/j.ijhydene.2021.05.059

Balde. (2018). *REPUBLIQUE DE GUINEE Travail-Justice-Solidarité MINISTERE DU PLAN ET DU DEVELOPPEMENT ECONOMIQUE La région de Kankan en chiffres*.

Barhoumi, E. M., Okonkwo, P. C., Ben Belgacem, I., Zghaibeh, M., & Tlili, I. (2022). *Optimal sizing of photovoltaic systems based green hydrogen refuelling stations case study Oman. International Journal of Hydrogen Energy*, *47*(75), 31964–31973. https://doi.org/10.1016/j.ijhydene.2022.07.140

Bhandari, B., Lee, K. T., Lee, G. Y., Cho, Y. M., & Ahn, S. H. (2015). *Optimization of hybrid renewable energy power systems:* A review. *International Journal of Precision Engineering and Manufacturing - Green Technology*, *2*(1), 99–112. https://doi.org/10.1007/s40684-015-0013-z

Calow, C., Macdonald, A. M., Nicol, A. L., & Robins, N. S. (2010). *Reconstruction of global gridded monthly sectoral water withdrawals for 1971-2010 and analysis of their spatiotemporal patterns.* In *JAWRA J. Am. Water Resour. Assoc* (Vol. 48, Issue 2). Macmillan College. https://theconversation.com/groundwater-reserves-in-africa-may-be-more-resilient-t

Caponi, R., Bocci, E., & Del Zotto, L. (2022). *Techno-Economic Model for Scaling Up of Hydrogen Refueling Stations. Energies*, *15*(20), 7518. https://doi.org/10.3390/en15207518

Caponi, R., Monforti Ferrario, A., Del Zotto, L., & Bocci, E. (2021a). *Hydrogen refueling station cost model applied to five real case studies for fuel cell buses. E3S Web of Conferences*, *312*, 07010. https://doi.org/10.1051/e3sconf/202131207010

Caponi, R., Monforti Ferrario, A., Del Zotto, L., & Bocci, E. (2021b). *Hydrogen refueling station cost model applied to five real case studies for fuel cell buses. E3S Web of Conferences*, *312*, 07010. https://doi.org/10.1051/e3sconf/202131207010

Contestabile, M., Offer, G. J., Slade, R., Jaeger, F., & Thoennes, M. (2011). *Battery electric vehicles, hydrogen fuel cells and biofuels. Which will be the winner? Energy & Environmental Science*, *4*(10), 3754. https://doi.org/10.1039/c1ee01804c

Conzade, J., Engel, H., Kendall, A., & Pais, G. (2022). *Power to move: Accelerating the electric transport transition in sub-Saharan Africa How governments,*

development partners, and private-sector stakeholders can build an enabling ecosystem for electric vehicles in the region.

Dadkhah, A., Bozalakov, D., De Kooning, J. D. M., & Vandevelde, L. (2021). *On the optimal planning of a hydrogen refuelling station participating in the electricity and balancing markets. International Journal of Hydrogen Energy*, *46*(2), 1488–1500. https://doi.org/10.1016/j.ijhydene.2020.10.130

De Blasio, N. (2021). *P A P E R The Role of Clean Hydrogen for a Sustainable Mobility*. www.belfercenter.org/ENRP

Deshmukh, M. K., & Deshmukh, S. S. (2008). *Modeling of hybrid renewable energy systems.* In *Renewable and Sustainable Energy Reviews* (Vol. 12, Issue 1, pp. 235–249). https://doi.org/10.1016/j.rser.2006.07.011

Di Micco, S., Minutillo, M., Perna, A., & Jannelli, E. (2022). *On-site solar powered refueling stations for green hydrogen production and distribution: performances and costs. E3S Web of Conferences*, *334*, 01005. https://doi.org/10.1051/e3sconf/202233401005

EDG. (n.d.). *SOCIETE ELECTRICITE DE GUINEE (EDG SA) TARIFS POST-PAIEMENT ET PRÉ-PAIEMENT.*

EERE. (2023). *ENERGY EFFICIENCY & RENEWABLE ENERGY (EERE) - HYDROGEN AND FUEL CELL TECHNOLOGIES OFFICE - Hydrogen Storage*. https://www.energy.gov/eere/fuelcells/hydrogen-storage

Emergence Guinée. (2019, February 28). *Transport : près de 40 mille véhicules sont immatriculés par an (ministre) – EmergenceGN.net*. https://emergencegn.net/guinee-pres-de-40-mille-vehicules-sont-immatricules-par-an-ministre-des-transports/

Encyclopaedia Britannica. (n.d.). *Kankan | Kankan | Traditional Culture, Handicrafts & Cuisine | Britannica | Written and fact-checked by The Editors of Encyclopaedia Britannica.* In *Britannica*.

EnergySage. (2022, November 30). *Clean Heating and Cooling Technologies | EnergySage*. https://www.energysage.com/clean-heating-

cooling/?_gl=1*1a15yqq*_gcl_au*MTY2MDEwODA2Ny4xNjg2MzQ1Mzc3

Ewing, M., Israel, B., Jutt, T., Talebian, H., & Stepanik, L. (2020). *Hydrogen on the path to net-zero emissions - Costs and climate benefits*. https://about.jstor.org/terms

Farzaneh-Gord, M., Deymi-Dashtebayaz, M., Rahbari, H. R., & Niazmand, H. (2012). *Effects of storage types and conditions on compressed hydrogen fuelling stations performance. International Journal of Hydrogen Energy*, *37*(4), 3500–3509. https://doi.org/10.1016/j.ijhydene.2011.11.017

Fragiacomo, P., & Genovese, M. (2020). *Developing a mathematical tool for hydrogen production, compression and storage. International Journal of Hydrogen Energy*, *45*(35), 17685–17701. https://doi.org/10.1016/j.ijhydene.2020.04.269

Global Solar Atlas. (n.d.). *Global Solar Atlas: Baté-Nafadji - 10.659706°, -009.24862° - N6, Baté-Nafadji, Kankan Region, Guinea - Time zone: UTC+00, Africa/Conakry [GMT] /Accessed on 01.08.2023 / https://globalsolaratlas.info/map?s=10.659706,-9.24862&m=site&c=10.659596,-9.248772,11*. Retrieved August 1, 2023, from https://globalsolaratlas.info/map?s=10.659706,-9.24862&m=site&c=10.659596,-9.248772,11

Global Wind Atlas. (n.d.). *Global Wind Atlas / Area: Guinea, Kankan Region*.

Gökçek, M. (2010). *Hydrogen generation from small-scale wind-powered electrolysis system in different power matching modes. International Journal of Hydrogen Energy*, *35*(19), 10050–10059. https://doi.org/10.1016/j.ijhydene.2010.07.149

Gökçek, M., & Kale, C. (2018a). *Optimal design of a Hydrogen Refuelling Station (HRFS) powered by Hybrid Power System. Energy Conversion and Management*, *161*, 215–224. https://doi.org/10.1016/j.enconman.2018.02.007

Gökçek, M., & Kale, C. (2018b). *Techno-economical evaluation of a hydrogen refuelling station powered by Wind-PV hybrid power system: A case study for*

İzmir-Çeşme. International Journal of Hydrogen Energy, *43*(23), 10615–10625. https://doi.org/10.1016/j.ijhydene.2018.01.082

Guinée Politique. (2021). *Guinée Politique - Présentation générale de la Guinée /https://guineepolitique.org/presentation-generale-de-la-guinee//Copyright © 2021. WATHI Think Tank/Web page visited on 28 July 2023*. https://www.mediaterre.org/afrique-ouest/actu,20130104162026.html

H2 Mobility. (2010). *H2 Mobility 1 70MPa HRS Standardization-Functional Description H2 Mobility 70MPa Hydrogen Refuelling Station Standardization Functional Description of Station Modules H2 Mobility 2 70MPa HRS Standardization-Functional Description V1.1 07-06-2010*.

Hammami, J. (2021, August 6). *Energy Capital & Power - Harnessing the Potential of Guinea Conakry's Renewable Energy - https://energycapitalpower.com/harnessing-the-potential-of-guinea-conakrys-renewable-energy-sector/*.

HOMERHelpManual. (2016). *HOMERHelpManual : HOMER Pro Version 3.7 - User Manual*.

Höök, M., & Tang, X. (2013). *Depletion of fossil fuels and anthropogenic climate change—*A review. *Energy Policy*, *52*, 797–809. https://doi.org/10.1016/j.enpol.2012.10.046

Hussain, S., Daneshmand, S. V., Zareipour, H., Layzell, D., & Khan, A. (2022). *Optimal Sizing of a Stand-alone Renewable-Powered Hydrogen Fueling Station. 2022 IEEE International Autumn Meeting on Power, Electronics and Computing, ROPEC 2022*. https://doi.org/10.1109/ROPEC55836.2022.10018821

HYDEVA. (n.d.). *H2 REFUELLING STATION | HYDEVA*. Retrieved July 8, 2023, from https://hydeva.com/hydrogen-refuelling-station/

IEA. (2020). *IEA (2020), Energy Technology Perspectives 2020, IEA, Paris.*

IEA. (2021a). *Global EV Outlook 2021, IEA, Paris https://www.iea.org/reports/global-ev-outlook-2021, License: CC BY 4.0*.

IEA. (2021b). *Global Hydrogen Review 2021, IEA, Paris https://www.iea.org/reports/global-hydrogen-review-2021, License: CC BY 4.0*.

IEA. (2022). *Global EV Outlook 2022, IEA, Paris https://www.iea.org/reports/global-ev-outlook-2022, License: CC BY 4.0*.

IEEE Staff, & IEEE Staff. (2012). *2012 IEEE/IAS Industrial and Commercial Power Systems Technical Conference.*

ITA. (2022, December 15). *Official Website of the International Trade Administration (ITA) - Guinea - Country Commercial Guide - Renewable Resources - https://www.trade.gov/country-commercial-guides/guinea-renewable-resources - Web page visited on 28 July 2023*.

Kavadias, K. A., Kosmas, V., & Tzelepis, S. (2022). *Sizing, Optimization, and Financial Analysis of a Green Hydrogen Refueling Station in Remote Regions. Energies*, *15*(2), 547. https://doi.org/10.3390/en15020547

Kebede, A. A., Coosemans, T., Messagie, M., Jemal, T., Behabtu, H. A., Van Mierlo, J., & Berecibar, M. (2021). *Techno-economic analysis of lithium-ion and lead-acid batteries in stationary energy storage application. Journal of Energy Storage*, *40*, 102748. https://doi.org/10.1016/j.est.2021.102748

Langiu, M., Shu, D. Y., Baader, F. J., Hering, D., Bau, U., Xhonneux, A., Müller, D., Bardow, A., Mitsos, A., & Dahmen, M. (2021). *COMANDO: A Next-Generation Open-Source Framework for Energy Systems Optimization. Computers & Chemical Engineering*, *152*, 107366. https://doi.org/10.1016/j.compchemeng.2021.107366

Médiaterre. (2013, January 4). *Fiche d'information sur les ressources en eau en Guinée - Médiaterre - Par Administrateur AGC, Modéré par Claude TOUTANT, Thématique(s) : Eau Rubrique : Contributions, depuis le 04/01/13 à 16h20 GMT*.

Micena, R. P., Llerena-Pizarro, O. R., de Souza, T. M., & Silveira, J. L. (2020). *Solar-powered Hydrogen Refueling Stations: A techno-economic analysis. International Journal of Hydrogen Energy*, *45*(3), 2308–2318. https://doi.org/10.1016/j.ijhydene.2019.11.092

Ministère de l'Énergie et de l'Hydraulique. (2012). *RÉPUBLIQUE DE GUINÉE/Ministère d'Etat Chargé de l'Énergie/PRESENTATION DU SECTEUR DE L'ENERGIE DE LA REPUBLIQUE DE GUINEE*.

Minutillo, M., Perna, A., Forcina, A., Di Micco, S., & Jannelli, E. (2021). *Analyzing the levelized cost of hydrogen in refueling stations with on-site hydrogen production via water electrolysis in the Italian scenario. International Journal of Hydrogen Energy*, *46*(26), 13667–13677. https://doi.org/10.1016/j.ijhydene.2020.11.110

Nistor, S., Dave, S., Fan, Z., & Sooriyabandara, M. (2016). *Technical and economic analysis of hydrogen refuelling. Applied Energy*, *167*, 211–220. https://doi.org/10.1016/j.apenergy.2015.10.094

NREL. (2022). *Technologies | Electricity | 2022 | ATB | NREL /Utility-Scale PV (https://atb.nrel.gov/electricity/2022/utility-scale_pv) / Utility-Scale Battery Storage (https://atb.nrel.gov/electricity/2022/utility-scale_battery_storage)*. https://atb.nrel.gov/electricity/2022/technologies

O'Toole, T. E. (2023). O'Toole, T. E. (2023, May 20). *Guinea. Encyclopedia Britannica.* https://www.britannica.com/place/Guinea. In *Encyclopædia Britannica, Inc.*

Pascal, T. (2022, May 31). *Overview of Grey, Blue, and Green Hydrogen*. https://www.structuresinsider.com/post/overview-of-grey-blue-and-green-hydrogen

Philips. (2023). *Philips lighting website: Inverter LED Lamp 9W CDL B22*. https://www.lighting.philips.co.in/search?page=1&query=inverter%20led%20lamp%209w%20cdl%20b22&size=12&page_type=productdetails

PLEUGER. (2023). *PLEUGER: Submersible Pumps*. https://www.pleugerindustries.com/en/products/submersible-pumps

PwC. (n.d.). *Green hydrogen economy - predicted development of tomorrow: PwC. Web page viewed on 12 July 2023*. Retrieved July 12, 2023, from https://www.pwc.com/gx/en/industries/energy-utilities-resources/future-energy/green-hydrogen-cost.html

Rabiee, A., Keane, A., & Soroudi, A. (2021). Green hydrogen: *A new flexibility source for security constrained scheduling of power systems with renewable energies. International Journal of Hydrogen Energy*, *46*(37), 19270–19284. https://doi.org/10.1016/j.ijhydene.2021.03.080

Radium.de. (2023). *Standard lamp, clear, A 60W/230/C/E27 | Radium.de (https://www.radium.de/en/products/standard-lamp-clear-60w230ce27)*. https://www.radium.de/en/products/standard-lamp-clear-60w230ce27

Ritchie, H. (2020, October 6). *Cars, planes, trains: where do CO2 emissions from transport come from? - Our World in Data*. https://ourworldindata.org/co2-emissions-from-transport

Sharma, D. K., Singh, B., Raja, M., Regin, R., & Rajest, S. S. (2021). *An Efficient Python Approach for Simulation of Poisson Distribution. 2021 7th International Conference on Advanced Computing and Communication Systems (ICACCS)*, 2011–2014. https://doi.org/10.1109/ICACCS51430.2021.9441895

SIE. (2023). *Systeme d'Information Energetique (SIE) Guinée / Ministere de l'Energie et de PHydraulique / Direction Nationale de l'Energie - Cellule SIE - Quartier Almamya – Commune de Kaloum, - BP: 1217 - Conakry/Guinée / https://www.sieguinee-dne.org/ministere-de-l-energie-et-de-l-hydraulique.html /.*

Stars, S., & Qin, N. (2014). *Hydrogen Fueling Stations Infrastructure Hydrogen Fueling Stations Infrastructure Florida Solar Energy Center*. http://library.ucf.edu

Stetson, N., & Department of Energy, U. (2021). *Dr. Ned Stetson, HFTO-Hydrogen Technologies Program Manager 2021 Annual Merit Review and Peer Evaluation Meeting H 2 Technologies Overview*.

Sun, W., & Harrison, G. P. (2021). *Active Load Management of Hydrogen Refuelling Stations for Increasing the Grid Integration of Renewable Generation. IEEE Access*, *9*, 101681–101694. https://doi.org/10.1109/ACCESS.2021.3098161

SYLLA, Y. (2022). *YOUSSOUF SYLLA Guinée Enjeux juridiques de la transition énergétique*.

Trading Economics. (2023). *Trading Economics: Guinea Interest Rate - 2023 Data - 2006-2022 Historical - 2024 Forecast - Chart - News*. 2023 Data - 2006-2022 Historical - 2024 Forecast - Chart - News. https://tradingeconomics.com/guinea/interest-rate

TWI. (2023). *TWI: WHAT IS HYDROGEN STORAGE AND HOW DOES IT WORK? https://www.twi-global.com/technical-knowledge/faqs/what-is-hydrogen-storage*. WHAT IS HYDROGEN STORAGE AND HOW DOES IT WORK? https://www.twi-global.com/technical-knowledge/faqs/what-is-hydrogen-storage

Urs, R. R., Chadly, A., Al Sumaiti, A., & Mayyas, A. (2023). *Techno-economic analysis of green hydrogen as an energy-storage medium for commercial buildings. Clean Energy*, *7*(1), 84–98. https://doi.org/10.1093/ce/zkac083

U.S. Department of Energy. (2019). *Office of Energy Efficiency & Renewable Energy, Fuel Cell Technologies Office: Increase your H2 IQ! https://www.energy.gov/sites/prod/files/2019/09/f67/fcto-increase-your-h2iq-training-resource-2019-update.pdf*.

WTO. (2011). *World Trade Organization (WTO) - Trade Policy Review of Guinea - WT/TPR/G/251* .

Xiao, J., Bénard, P., & Chahine, R. (2016). *Charge-discharge cycle thermodynamics for compression hydrogen storage system. International Journal of Hydrogen Energy*, *41*(12), 5531–5539. https://doi.org/10.1016/j.ijhydene.2015.12.136

Xiao, J., Ma, S., Wang, X., Deng, S., Yang, T., & Bénard, P. (2019). *Effect of Hydrogen Refueling Parameters on Final State of Charge. Energies*, *12*(4), 645. https://doi.org/10.3390/en12040645

Xu, Z., Dong, W., Yang, K., Zhao, Y., & He, G. (2022). *Development of efficient hydrogen refueling station by process optimization and control. International Journal of Hydrogen Energy*, *47*(56), 23721–23730. https://doi.org/10.1016/j.ijhydene.2022.05.158

Yohannes, B., & Diedou, A. (2022, July 13). *Green hydrogen: A viable option for transforming Africa's energy sector | Africa Renewal*.

https://www.un.org/africarenewal/magazine/july-2022/green-hydrogen-viable-option-transforming-africas-energy-sector

Zhang, H., Su, S., Lin, G., & Chen, J. (2012). *Efficiency Calculation and Configuration Design of a PEM Electrolyzer System for Hydrogen Production.* In *Int. J. Electrochem. Sci* (Vol. 7). www.electrochemsci.org

Appendices

Appendix 1: Electricity generation and demand profiles within the grid-connected PV system

t	Typical days	Weights	PV	El. From Grid [kWh]	Electrolyser [kWh]	Compressor [kWh]	HRS loads [kWh]	El. To Grid [kWh]
0	27	1	0	1.04	0	0	1.04	0
1	27	1	0	1.04	0	0	1.04	0
2	27	1	0	1.04	0	0	1.04	0
3	27	1	0	1.04	0	0	1.04	0
4	27	1	0	1.04	0	0	1.04	0
5	27	1	0	1.04	0	0	1.04	0
6	27	1	0	18.15	0	0	18.15	0
7	27	1	1078.04	0	935.3	67.65	33.6	34.36
8	27	1	1327.72	0	1184.98	85.7	49.9	0
9	27	1	1387.18	0	1244.45	90	44.15	1.44
10	27	1	1387.18	0	1244.45	90	44.15	1.44
11	27	1	204.21	0	61.47	4.45	131.15	0
12	27	1	956.37	0	813.63	58.85	76.75	0
13	27	1	1331.06	0	1188.33	85.95	49.65	0
14	27	1	1181.74	0	1039	75.15	60.45	0
15	27	1	1181.74	0	1039	75.15	60.45	0
16	27	1	974.49	0	831.76	60.16	49.65	25.79
17	27	1	559.36	0	416.63	30.13	44.15	61.31
18	27	1	14.47	14.72	0	0	28.47	0
19	27	1	0	61.31	0	0	61.31	0
20	27	1	0	83.71	0	0	83.71	0
21	27	1	0	50.75	0	0	50.75	0
22	27	1	0	50.75	0	0	50.75	0
23	27	1	0	1.04	0	0	1.04	0
24	37	72.6	0	1.04	0	0	1.04	0
25	37	72.6	0	1.04	0	0	1.04	0
26	37	72.6	0	1.04	0	0	1.04	0
27	37	72.6	0	1.04	0	0	1.04	0
28	37	72.6	0	1.04	0	0	1.04	0
29	37	72.6	0	1.04	0	0	1.04	0
30	37	72.6	0	18.15	0	0	18.15	0
31	37	72.6	788.63	0	645.9	46.71	33.6	55.29
32	37	72.6	1327.72	0	1184.98	85.7	49.9	0
33	37	72.6	1387.18	0	1244.45	90	44.15	1.44
34	37	72.6	1387.18	0	1244.45	90	44.15	1.44
35	37	72.6	204.21	0	61.47	4.45	131.15	0

t	Typical days	Weights	PV	El. From Grid [kWh]	Electrolyser [kWh]	Compressor [kWh]	HRS loads [kWh]	El. To Grid [kWh]
35	37	72.6	204.21	0	61.47	4.45	131.15	0
36	37	72.6	956.37	0	813.63	58.85	76.75	0
37	37	72.6	1331.06	0	1188.33	85.95	49.65	0
38	37	72.6	1181.74	0	1039	75.15	60.45	0
39	37	72.6	1181.74	0	1039	75.15	60.45	0
40	37	72.6	1263.9	0	1121.17	81.09	49.65	4.86
41	37	72.6	559.36	0	416.63	30.13	44.15	61.31
42	37	72.6	14.47	14.72	0	0	28.47	0
43	37	72.6	0	61.31	0	0	61.31	0
44	37	72.6	0	83.71	0	0	83.71	0
45	37	72.6	0	50.75	0	0	50.75	0
46	37	72.6	0	50.75	0	0	50.75	0
47	37	72.6	0	1.04	0	0	1.04	0
48	71	48.73	0	1.04	0	0	1.04	0
49	71	48.73	0	1.04	0	0	1.04	0
50	71	48.73	0	1.04	0	0	1.04	0
51	71	48.73	0	1.04	0	0	1.04	0
52	71	48.73	0	1.04	0	0	1.04	0
53	71	48.73	0	1.04	0	0	1.04	0
54	71	48.73	0	18.15	0	0	18.15	0
55	71	48.73	658.4	0	515.66	37.3	33.6	64.71
56	71	48.73	1327.72	0	1184.98	85.7	49.9	0
57	71	48.73	1387.18	0	1244.45	90	44.15	1.44
58	71	48.73	1387.18	0	1244.45	90	44.15	1.44
59	71	48.73	204.21	0	61.47	4.45	131.15	0
60	71	48.73	956.37	0	813.63	58.85	76.75	0
61	71	48.73	1331.06	0	1188.33	85.95	49.65	0
62	71	48.73	1181.74	0	1039	75.15	60.45	0
63	71	48.73	1181.74	0	1039	75.15	60.45	0
64	71	48.73	1331.06	0	1188.33	85.95	49.65	0
65	71	48.73	622.43	0	479.7	34.69	44.15	56.75
66	71	48.73	28.94	0.97	0	0	28.47	0
67	71	48.73	0	61.31	0	0	61.31	0
68	71	48.73	0	83.71	0	0	83.71	0
69	71	48.73	0	50.75	0	0	50.75	0
70	71	48.73	0	50.75	0	0	50.75	0
71	71	48.73	0	1.04	0	0	1.04	0
72	85	45.75	0	1.04	0	0	1.04	0
73	85	45.75	0	1.04	0	0	1.04	0
74	85	45.75	0	1.04	0	0	1.04	0
75	85	45.75	0	1.04	0	0	1.04	0

t	Typical days	Weights	PV	El. From Grid [kWh]	Electrolyser [kWh]	Compressor [kWh]	HRS loads [kWh]	El. To Grid [kWh]
75	85	45.75	0	1.04	0	0	1.04	0
76	85	45.75	0	1.04	0	0	1.04	0
77	85	45.75	0	1.04	0	0	1.04	0
78	85	45.75	0	18.15	0	0	18.15	0
79	85	45.75	723.52	0	580.78	42.01	33.6	60
80	85	45.75	1327.72	0	1184.98	85.7	49.9	0
81	85	45.75	1387.18	0	1244.45	90	44.15	1.44
82	85	45.75	1387.18	0	1244.45	90	44.15	1.44
83	85	45.75	204.21	0	61.47	4.45	131.15	0
84	85	45.75	956.37	0	813.63	58.85	76.75	0
85	85	45.75	1331.06	0	1188.33	85.95	49.65	0
86	85	45.75	1181.74	0	1039	75.15	60.45	0
87	85	45.75	1181.74	0	1039	75.15	60.45	0
88	85	45.75	1329.02	0	1186.28	85.8	49.65	0.15
89	85	45.75	559.36	0	416.63	30.13	44.15	61.31
90	85	45.75	36.18	0	0	0	28.47	5.9
91	85	45.75	0	61.31	0	0	61.31	0
92	85	45.75	0	83.71	0	0	83.71	0
93	85	45.75	0	50.75	0	0	50.75	0
94	85	45.75	0	50.75	0	0	50.75	0
95	85	45.75	0	1.04	0	0	1.04	0
96	87	36.8	0	1.04	0	0	1.04	0
97	87	36.8	0	1.04	0	0	1.04	0
98	87	36.8	0	1.04	0	0	1.04	0
99	87	36.8	0	1.04	0	0	1.04	0
100	87	36.8	0	1.04	0	0	1.04	0
101	87	36.8	0	1.04	0	0	1.04	0
102	87	36.8	0	18.15	0	0	18.15	0
103	87	36.8	600.52	0	457.78	33.11	33.6	68.89
104	87	36.8	1327.72	0	1184.98	85.7	49.9	0
105	87	36.8	1387.18	0	1244.45	90	44.15	1.44
106	87	36.8	1387.18	0	1244.45	90	44.15	1.44
107	87	36.8	204.21	0	61.47	4.45	131.15	0
108	87	36.8	956.37	0	813.63	58.85	76.75	0
109	87	36.8	1331.06	0	1188.33	85.95	49.65	0
110	87	36.8	1181.74	0	1039	75.15	60.45	0
111	87	36.8	1181.74	0	1039	75.15	60.45	0
112	87	36.8	1331.06	0	1188.33	85.95	49.65	0
113	87	36.8	680.31	0	537.58	38.88	44.15	52.57
114	87	36.8	43.41	0	0	0	28.47	12.77
115	87	36.8	0	61.31	0	0	61.31	0

t	Typical days	Weights	PV	El. From Grid [kWh]	Electrolyser [kWh]	Compressor [kWh]	HRS loads [kWh]	El. To Grid [kWh]
115	87	36.8	0	61.31	0	0	61.31	0
116	87	36.8	0	83.71	0	0	83.71	0
117	87	36.8	0	50.75	0	0	50.75	0
118	87	36.8	0	50.75	0	0	50.75	0
119	87	36.8	0	1.04	0	0	1.04	0
120	107	36.8	0	1.04	0	0	1.04	0
121	107	36.8	0	1.04	0	0	1.04	0
122	107	36.8	0	1.04	0	0	1.04	0
123	107	36.8	0	1.04	0	0	1.04	0
124	107	36.8	0	1.04	0	0	1.04	0
125	107	36.8	0	1.04	0	0	1.04	0
126	107	36.8	21.71	0	0	0	18.15	2.47
127	107	36.8	803.1	0	660.37	47.76	33.6	54.24
128	107	36.8	1246.08	0	1103.35	79.8	49.9	5.9
129	107	36.8	1387.18	0	1244.45	90	44.15	1.44
130	107	36.8	1387.18	0	1244.45	90	44.15	1.44
131	107	36.8	204.21	0	61.47	4.45	131.15	0
132	107	36.8	956.37	0	813.63	58.85	76.75	0
133	107	36.8	1331.06	0	1188.33	85.95	49.65	0
134	107	36.8	1181.74	0	1039	75.15	60.45	0
135	107	36.8	1181.74	0	1039	75.15	60.45	0
136	107	36.8	1331.06	0	1188.33	85.95	49.65	0
137	107	36.8	559.36	0	416.63	30.13	44.15	61.31
138	107	36.8	72.35	0	0	0	28.47	40.27
139	107	36.8	0	61.31	0	0	61.31	0
140	107	36.8	0	83.71	0	0	83.71	0
141	107	36.8	0	50.75	0	0	50.75	0
142	107	36.8	0	50.75	0	0	50.75	0
143	107	36.8	0	1.04	0	0	1.04	0
144	180	40.78	0	1.04	0	0	1.04	0
145	180	40.78	0	1.04	0	0	1.04	0
146	180	40.78	0	1.04	0	0	1.04	0
147	180	40.78	0	1.04	0	0	1.04	0
148	180	40.78	0	1.04	0	0	1.04	0
149	180	40.78	0	1.04	0	0	1.04	0
150	180	40.78	50.65	0	0	0	18.15	29.96
151	180	40.78	803.1	0	660.37	47.76	33.6	54.24
152	180	40.78	1327.72	0	1184.98	85.7	49.9	0
153	180	40.78	1387.18	0	1244.45	90	44.15	1.44
154	180	40.78	1387.18	0	1244.45	90	44.15	1.44
155	180	40.78	204.21	0	61.47	4.45	131.15	0

t	Typical days	Weights	PV	El. From Grid [kWh]	Electrolyser [kWh]	Compressor [kWh]	HRS loads [kWh]	El. To Grid [kWh]
155	180	40.78	204.21	0	61.47	4.45	131.15	0
156	180	40.78	956.37	0	813.63	58.85	76.75	0
157	180	40.78	1331.06	0	1188.33	85.95	49.65	0
158	180	40.78	1181.74	0	1039	75.15	60.45	0
159	180	40.78	1181.74	0	1039	75.15	60.45	0
160	180	40.78	1273.39	0	1130.65	81.77	49.65	4.17
161	180	40.78	535.4	0	392.67	28.4	44.15	63.05
162	180	40.78	65.12	0	0	0	28.47	33.39
163	180	40.78	0	61.31	0	0	61.31	0
164	180	40.78	0	83.71	0	0	83.71	0
165	180	40.78	0	50.75	0	0	50.75	0
166	180	40.78	0	50.75	0	0	50.75	0
167	180	40.78	0	1.04	0	0	1.04	0
168	202	1	0	1.04	0	0	1.04	0
169	202	1	0	1.04	0	0	1.04	0
170	202	1	0	1.04	0	0	1.04	0
171	202	1	0	1.04	0	0	1.04	0
172	202	1	0	1.04	0	0	1.04	0
173	202	1	0	1.04	0	0	1.04	0
174	202	1	0	18.15	0	0	18.15	0
175	202	1	130.23	43.01	130.23	9.42	33.6	0
176	202	1	390.7	78.15	390.7	28.26	49.9	0
177	202	1	737.99	97.53	737.99	53.38	44.15	0
178	202	1	976.75	114.8	976.75	70.64	44.15	0
179	202	1	1172.1	215.93	1172.1	84.77	131.15	0
180	202	1	1244.45	166.76	1244.45	90	76.75	0
181	202	1	1266.15	119.04	1244.45	90	49.65	0
182	202	1	1208.27	147.84	1208.27	87.39	60.45	0
183	202	1	1128.69	142.09	1128.69	81.63	60.45	0
184	202	1	991.22	121.34	991.22	71.69	49.65	0
185	202	1	651.16	91.25	651.16	47.1	44.15	0
186	202	1	123	37.36	123	8.9	28.47	0
187	202	1	0	61.31	0	0	61.31	0
188	202	1	0	83.71	0	0	83.71	0
189	202	1	0	50.75	0	0	50.75	0
190	202	1	0	50.75	0	0	50.75	0
191	202	1	0	1.04	0	0	1.04	0
192	258	45.75	0	1.04	0	0	1.04	0
193	258	45.75	0	1.04	0	0	1.04	0
194	258	45.75	0	1.04	0	0	1.04	0
195	258	45.75	0	1.04	0	0	1.04	0

t	Typical days	Weights	PV	El. From Grid [kWh]	Electrolyser [kWh]	Compressor [kWh]	HRS loads [kWh]	El. To Grid [kWh]
195	258	45.75	0	1.04	0	0	1.04	0
196	258	45.75	0	1.04	0	0	1.04	0
197	258	45.75	0	1.04	0	0	1.04	0
198	258	45.75	0	18.15	0	0	18.15	0
199	258	45.75	332.82	0	276.41	19.99	33.6	0
200	258	45.75	1020.16	0	899.18	65.03	49.9	0
201	258	45.75	1387.18	0	1244.45	90	44.15	1.44
202	258	45.75	1387.18	0	1244.45	90	44.15	1.44
203	258	45.75	489.25	20.62	346.51	25.06	131.15	0
204	258	45.75	975.99	1.42	833.25	60.26	76.75	0
205	258	45.75	1387.18	4.06	1244.45	90	49.65	0
206	258	45.75	1181.74	0	1039	75.15	60.45	0
207	258	45.75	1181.74	0	1039	75.15	60.45	0
208	258	45.75	1387.18	4.06	1244.45	90	49.65	0
209	258	45.75	665.64	0	575.36	41.61	44.15	0
210	258	45.75	43.41	0	12.49	0.9	28.47	0
211	258	45.75	0	61.31	0	0	61.31	0
212	258	45.75	0	83.71	0	0	83.71	0
213	258	45.75	0	50.75	0	0	50.75	0
214	258	45.75	0	50.75	0	0	50.75	0
215	258	45.75	0	1.04	0	0	1.04	0
216	285	35.8	0	1.04	0	0	1.04	0
217	285	35.8	0	1.04	0	0	1.04	0
218	285	35.8	0	1.04	0	0	1.04	0
219	285	35.8	0	1.04	0	0	1.04	0
220	285	35.8	0	1.04	0	0	1.04	0
221	285	35.8	0	1.04	0	0	1.04	0
222	285	35.8	0	18.15	0	0	18.15	0
223	285	35.8	368.99	0	310.03	22.42	33.6	0
224	285	35.8	1324.04	0	1181.56	85.46	49.9	0
225	285	35.8	1387.18	0	1244.45	90	44.15	1.44
226	285	35.8	1387.18	0	1244.45	90	44.15	1.44
227	285	35.8	860.22	47.45	717.48	51.89	131.15	0
228	285	35.8	975.99	1.42	833.25	60.26	76.75	0
229	285	35.8	1387.18	4.06	1244.45	90	49.65	0
230	285	35.8	1181.74	0	1039	75.15	60.45	0
231	285	35.8	1181.74	0	1039	75.15	60.45	0
232	285	35.8	1005.69	0	885.97	64.08	49.65	0
233	285	35.8	325.58	0	259.36	18.76	44.15	0
234	285	35.8	0	28.47	0	0	28.47	0
235	285	35.8	0	61.31	0	0	61.31	0

t	Typical days	Weights	PV	El. From Grid [kWh]	Electrolyser [kWh]	Compressor [kWh]	HRS loads [kWh]	El. To Grid [kWh]
235	285	35.8	0	61.31	0	0	61.31	0
236	285	35.8	0	83.71	0	0	83.71	0
237	285	35.8	0	50.75	0	0	50.75	0
238	285	35.8	0	50.75	0	0	50.75	0
239	285	35.8	0	1.04	0	0	1.04	0

Appendix 2: Hydrogen production, storage, de-storage, and refuelling for grid-connected PV system

No.	Scenarios	Weights	Electrolyser output	H2 tank output	H2 tank input	FCEVs fuelling
1	27	1	0	0	0	0
2	27	1	0	0	0	0
3	27	1	0	0	0	0
4	27	1	0	0	0	0
5	27	1	0	0	0	0
6	27	1	0	0	0	0
7	27	1	0	166.65	0	166.65
8	27	1	748.24	0	414.94	333.3
9	27	1	947.99	0	448.04	499.95
10	27	1	995.56	0	662.26	333.3
11	27	1	995.56	0	662.26	333.3
12	27	1	49.18	1117.37	0	1166.55
13	27	1	650.9	15.7	0	666.6
14	27	1	950.66	0	617.36	333.3
15	27	1	831.2	0	331.25	499.95
16	27	1	831.2	0	331.25	499.95
17	27	1	665.41	0	332.11	333.3
18	27	1	333.3	0	0	333.3
19	27	1	0	166.65	0	166.65
20	27	1	0	499.95	0	499.95
21	27	1	0	833.25	0	833.25
22	27	1	0	499.95	0	499.95
23	27	1	0	499.95	0	499.95
24	27	1	0	0	0	0
25	37	72.6	0	0	0	0
26	37	72.6	0	0	0	0
27	37	72.6	0	0	0	0
28	37	72.6	0	0	0	0
29	37	72.6	0	0	0	0

No.	Scenarios	Weights	Electrolyser output	H2 tank output	H2 tank input	FCEVs fuelling
29	37	72.6	0	0	0	0
30	37	72.6	0	0	0	0
31	37	72.6	0	166.65	0	166.65
32	37	72.6	516.72	0	183.42	333.3
33	37	72.6	947.99	0	448.04	499.95
34	37	72.6	995.56	0	662.26	333.3
35	37	72.6	995.56	0	662.26	333.3
36	37	72.6	49.18	1117.37	0	1166.55
37	37	72.6	650.9	15.7	0	666.6
38	37	72.6	950.66	0	617.36	333.3
39	37	72.6	831.2	0	331.25	499.95
40	37	72.6	831.2	0	331.25	499.95
41	37	72.6	896.93	0	563.63	333.3
42	37	72.6	333.3	0	0	333.3
43	37	72.6	0	166.65	0	166.65
44	37	72.6	0	499.95	0	499.95
45	37	72.6	0	833.25	0	833.25
46	37	72.6	0	499.95	0	499.95
47	37	72.6	0	499.95	0	499.95
48	37	72.6	0	0	0	0
49	71	48.73	0	0	0	0
50	71	48.73	0	0	0	0
51	71	48.73	0	0	0	0
52	71	48.73	0	0	0	0
53	71	48.73	0	0	0	0
54	71	48.73	0	0	0	0
55	71	48.73	0	166.65	0	166.65
56	71	48.73	412.53	0	79.23	333.3
57	71	48.73	947.99	0	448.04	499.95
58	71	48.73	995.56	0	662.26	333.3
59	71	48.73	995.56	0	662.26	333.3
60	71	48.73	49.18	1117.37	0	1166.55
61	71	48.73	650.9	15.7	0	666.6
62	71	48.73	950.66	0	617.36	333.3
63	71	48.73	831.2	0	331.25	499.95
64	71	48.73	831.2	0	331.25	499.95
65	71	48.73	950.66	0	617.36	333.3
66	71	48.73	383.76	0	50.46	333.3
67	71	48.73	0	166.65	0	166.65
68	71	48.73	0	499.95	0	499.95
69	71	48.73	0	833.25	0	833.25
70	71	48.73	0	499.95	0	499.95

No.	Scenarios	Weights	Electrolyser output	H2 tank output	H2 tank input	FCEVs fuelling
70	71	48.73	0	499.95	0	499.95
71	71	48.73	0	499.95	0	499.95
72	71	48.73	0	0	0	0
73	85	45.75	0	0	0	0
74	85	45.75	0	0	0	0
75	85	45.75	0	0	0	0
76	85	45.75	0	0	0	0
77	85	45.75	0	0	0	0
78	85	45.75	0	0	0	0
79	85	45.75	0	166.65	0	166.65
80	85	45.75	464.62	0	131.32	333.3
81	85	45.75	947.99	0	448.04	499.95
82	85	45.75	995.56	0	662.26	333.3
83	85	45.75	995.56	0	662.26	333.3
84	85	45.75	49.18	1117.37	0	1166.55
85	85	45.75	650.9	15.7	0	666.6
86	85	45.75	950.66	0	617.36	333.3
87	85	45.75	831.2	0	331.25	499.95
88	85	45.75	831.2	0	331.25	499.95
89	85	45.75	949.03	0	615.73	333.3
90	85	45.75	333.3	0	0	333.3
91	85	45.75	0	166.65	0	166.65
92	85	45.75	0	499.95	0	499.95
93	85	45.75	0	833.25	0	833.25
94	85	45.75	0	499.95	0	499.95
95	85	45.75	0	499.95	0	499.95
96	85	45.75	0	0	0	0
97	87	36.8	0	0	0	0
98	87	36.8	0	0	0	0
99	87	36.8	0	0	0	0
100	87	36.8	0	0	0	0
101	87	36.8	0	0	0	0
102	87	36.8	0	0	0	0
103	87	36.8	0	166.65	0	166.65
104	87	36.8	366.23	0	32.93	333.3
105	87	36.8	947.99	0	448.04	499.95
106	87	36.8	995.56	0	662.26	333.3
107	87	36.8	995.56	0	662.26	333.3
108	87	36.8	49.18	1117.37	0	1166.55
109	87	36.8	650.9	15.7	0	666.6
110	87	36.8	950.66	0	617.36	333.3
111	87	36.8	831.2	0	331.25	499.95

No.	Scenarios	Weights	Electrolyser output	H2 tank output	H2 tank input	FCEVs fuelling
111	87	36.8	831.2	0	331.25	499.95
112	87	36.8	831.2	0	331.25	499.95
113	87	36.8	950.66	0	617.36	333.3
114	87	36.8	430.06	0	96.76	333.3
115	87	36.8	0	166.65	0	166.65
116	87	36.8	0	499.95	0	499.95
117	87	36.8	0	833.25	0	833.25
118	87	36.8	0	499.95	0	499.95
119	87	36.8	0	499.95	0	499.95
120	87	36.8	0	0	0	0
121	107	36.8	0	0	0	0
122	107	36.8	0	0	0	0
123	107	36.8	0	0	0	0
124	107	36.8	0	0	0	0
125	107	36.8	0	0	0	0
126	107	36.8	0	0	0	0
127	107	36.8	0	166.65	0	166.65
128	107	36.8	528.29	0	194.99	333.3
129	107	36.8	882.68	0	382.73	499.95
130	107	36.8	995.56	0	662.26	333.3
131	107	36.8	995.56	0	662.26	333.3
132	107	36.8	49.18	1117.37	0	1166.55
133	107	36.8	650.9	15.7	0	666.6
134	107	36.8	950.66	0	617.36	333.3
135	107	36.8	831.2	0	331.25	499.95
136	107	36.8	831.2	0	331.25	499.95
137	107	36.8	950.66	0	617.36	333.3
138	107	36.8	333.3	0	0	333.3
139	107	36.8	0	166.65	0	166.65
140	107	36.8	0	499.95	0	499.95
141	107	36.8	0	833.25	0	833.25
142	107	36.8	0	499.95	0	499.95
143	107	36.8	0	499.95	0	499.95
144	107	36.8	0	0	0	0
145	180	40.78	0	0	0	0
146	180	40.78	0	0	0	0
147	180	40.78	0	0	0	0
148	180	40.78	0	0	0	0
149	180	40.78	0	0	0	0
150	180	40.78	0	0	0	0
151	180	40.78	0	166.65	0	166.65
152	180	40.78	528.29	0	194.99	333.3

X

No.	Scenarios	Weights	Electrolyser output	H2 tank output	H2 tank input	FCEVs fuelling
152	180	40.78	528.29	0	194.99	333.3
153	180	40.78	947.99	0	448.04	499.95
154	180	40.78	995.56	0	662.26	333.3
155	180	40.78	995.56	0	662.26	333.3
156	180	40.78	49.18	1117.37	0	1166.55
157	180	40.78	650.9	15.7	0	666.6
158	180	40.78	950.66	0	617.36	333.3
159	180	40.78	831.2	0	331.25	499.95
160	180	40.78	831.2	0	331.25	499.95
161	180	40.78	904.52	0	571.22	333.3
162	180	40.78	314.13	19.17	0	333.3
163	180	40.78	0	166.65	0	166.65
164	180	40.78	0	499.95	0	499.95
165	180	40.78	0	833.25	0	833.25
166	180	40.78	0	499.95	0	499.95
167	180	40.78	0	499.95	0	499.95
168	180	40.78	0	0	0	0
169	202	1	0	0	0	0
170	202	1	0	0	0	0
171	202	1	0	0	0	0
172	202	1	0	0	0	0
173	202	1	0	0	0	0
174	202	1	0	0	0	0
175	202	1	0	166.65	0	166.65
176	202	1	104.19	229.11	0	333.3
177	202	1	312.56	187.39	0	499.95
178	202	1	590.39	0	257.09	333.3
179	202	1	781.4	0	448.1	333.3
180	202	1	937.68	228.87	0	1166.55
181	202	1	995.56	0	328.96	666.6
182	202	1	995.56	0	662.26	333.3
183	202	1	966.62	0	466.67	499.95
184	202	1	902.95	0	403	499.95
185	202	1	792.97	0	459.67	333.3
186	202	1	520.93	0	187.63	333.3
187	202	1	98.4	68.25	0	166.65
188	202	1	0	499.95	0	499.95
189	202	1	0	833.25	0	833.25
190	202	1	0	499.95	0	499.95
191	202	1	0	499.95	0	499.95
192	202	1	0	0	0	0
193	258	45.75	0	0	0	0

No.	Scenarios	Weights	Electrolyser output	H2 tank output	H2 tank input	FCEVs fuelling
193	258	45.75	0	0	0	0
194	258	45.75	0	0	0	0
195	258	45.75	0	0	0	0
196	258	45.75	0	0	0	0
197	258	45.75	0	0	0	0
198	258	45.75	0	0	0	0
199	258	45.75	0	166.65	0	166.65
200	258	45.75	221.13	112.17	0	333.3
201	258	45.75	719.34	0	219.39	499.95
202	258	45.75	995.56	0	662.26	333.3
203	258	45.75	995.56	0	662.26	333.3
204	258	45.75	277.21	889.34	0	1166.55
205	258	45.75	666.6	0	0	666.6
206	258	45.75	995.56	0	662.26	333.3
207	258	45.75	831.2	0	331.25	499.95
208	258	45.75	831.2	0	331.25	499.95
209	258	45.75	995.56	0	662.26	333.3
210	258	45.75	460.28	0	126.98	333.3
211	258	45.75	9.99	156.66	0	166.65
212	258	45.75	0	499.95	0	499.95
213	258	45.75	0	833.25	0	833.25
214	258	45.75	0	499.95	0	499.95
215	258	45.75	0	499.95	0	499.95
216	258	45.75	0	0	0	0
217	285	35.8	0	0	0	0
218	285	35.8	0	0	0	0
219	285	35.8	0	0	0	0
220	285	35.8	0	0	0	0
221	285	35.8	0	0	0	0
222	285	35.8	0	0	0	0
223	285	35.8	0	166.65	0	166.65
224	285	35.8	248.02	85.28	0	333.3
225	285	35.8	945.25	0	445.3	499.95
226	285	35.8	995.56	0	662.26	333.3
227	285	35.8	995.56	0	662.26	333.3
228	285	35.8	573.99	592.56	0	1166.55
229	285	35.8	666.6	0	0	666.6
230	285	35.8	995.56	0	662.26	333.3
231	285	35.8	831.2	0	331.25	499.95
232	285	35.8	831.2	0	331.25	499.95
233	285	35.8	708.78	0	375.48	333.3
234	285	35.8	207.49	125.81	0	333.3

No.	Scenarios	Weights	Electrolyser output	H2 tank output	H2 tank input	FCEVs fuelling
234	285	35.8	207.49	125.81	0	333.3
235	285	35.8	0	166.65	0	166.65
236	285	35.8	0	499.95	0	499.95
237	285	35.8	0	833.25	0	833.25
238	285	35.8	0	499.95	0	499.95
239	285	35.8	0	499.95	0	499.95
240	285	35.8	0	0	0	0